

**THE APPLICATION OF SATELLITE BASED
PRECIPITATION FOR FLOOD INUNDATION MAPPING
OF MIDDLE INDUS BASIN**



By

Muhammad Majid

2010-NUST-MS PhD-GIS-12

**A thesis submitted in partial fulfillment of the requirements for the
degree of Master of Science in Remote Sensing and GIS**

**Institute of Geographical Information Systems
School of Civil and Environmental Engineering
National University of Sciences & Technology
Islamabad, Pakistan**

June, 2014

CERTIFICATE

Certified that the contents and form of thesis entitled “**The Application of Satellite Based Precipitation for Flood Inundation Mapping of Middle Indus Basin**” submitted by Mr. Muhammad Majid have been found satisfactory for the requirement of Master of Science degree in Remote Sensing and Geographical Information Systems.

Supervisor: _____

Professor Dr. Muhammad Umar Khan Khattak

Head of Department, IGIS

SCEE, NUST

Member: _____

Dr. Ejaz Hussain

Associate Dean, IGIS

SCEE, NUST

Member: _____

Dr. Ali Tahir

Assistant Professor, IGIS

SCEE, NUST

Member: _____

Mr. Azmat Hayat Khan

Director PMD, Islamabad

ACADEMIC THESIS: DECLARATION OF AUTHORSHIP

I, Muhammad Majid, declare that this thesis and the work presented in it are my own and have been generated by me as the result of my own original research.

The Application of Satellite based Precipitation for Flood Inundation

Mapping of Middle Indus Basin

I conform that:

1. This work was done wholly by me in candidature for an MS research degree at the National University of Sciences and Technology, Islamabad.
2. Wherever I have consulted the published work of others, it has been clearly attributed.
3. Wherever I have quoted from the work of others, the source has been always cited. With the exception of such quotations, this thesis is entirely my own.
4. I have acknowledged all main sources of help.
5. Where the work of thesis is based on work done by myself jointly with others, I have made clear exactly what was done by others and what I have contributed myself.
6. None of this work has been published before submission. This work is not plagiarized under the HEC plagiarism policy.

Signed:

Date:

DEDICATION

To my Parents

ACKNOWLEDGEMENTS

I would like to thank the following people and organizations whose valuable help and assistance have made the completion of this study possible.

Professor Dr. Muhammad Umar Khan Khattak, my supervisor, for providing generous support to pursue trainings for professional development and for ensuring that I finish the thesis according to the schedule. I am also thankful for his continuous encouragement, perpetual guidance, thoughtful suggestions and constructive criticism during the entire dissertation period. He was a constant source of inspiration and encouragement throughout my research.

I want to give credit to my GEC members specially Mr. Azmat Hayat Khan, Director PMD, Islamabad for his continuous assistance and guidance on my thesis. His ideas during data collection, processing and analysis enabled me to refine my work.

I would like to acknowledge Pakistan Metrological Department Islamabad for providing me rainfall data, Climate Data Processing Center Karachi for providing climatic data for the years 2003-2012 and Flood Forecasting Commission Islamabad for providing stream flow data on daily basis from 2003-2012 is highly appreciated. This research was possible with the generous research fund provided by NUST.

I am also thankful to all my class fellows, friends, colleagues and family members for their sincere attitude, moral support and prayers which inspired me every moment towards successful completion of my research.

Muhammad Majid

TABLE OF CONTENTS

CERTIFICATE	I
ACADEMIC THESIS: DECLARATION OF AUTHORSHIP	II
DEDICATION	III
ACKNOWLEDGEMENTS	IV
LIST OF FIGURES.....	VII
LIST OF TABLE	X
LIST OF ABBREVIATIONS	XII
ABSTRACT.....	XIII
INTRODUCTION.....	1
1.1 BACKGROUND	1
1.2 RATIONALE.....	3
1.3 OBJECTIVES	3
1.4 STUDY AREA	4
1.5 CLIMATE.....	4
1.6 RAINFALL.....	4
1.7 HYDROLOGY	6
1.8 AGRICULTURE	6
1.9 SCOPE OF THE STUDY	7
REVIEW OF LITRATURE.....	8
2.1 Precipitation and its measurement	8
2.2 rain gauges Types	8
2.2.1. Non-Recording Gauge	8
2.2.2. Recording Gauges.....	10
2.3 error in rain gauge MEASUREMENT	11
2.3.1 Wind-Induced Errors	11
2.3.2 Evaporation and Wetting Loss.....	13
2.3.3 Calibration Errors.....	13
2.3.4 Other errors in rain gauge measurements	13
2.4 Satellite based precipitation estimates	13
2.5 Overview of satellite precipitation data	14
2.6 Tropical Rainfall Measuring Mission	15
2.6.1 Introduction.....	15
2.6.2 Precipitation Radar (PR).....	15
2.6.3 TRMM Microwave Imager (TMI).....	17
2.6.4 Visible and Infrared Scanner (VIRS).....	18
2.6.5 Clouds and the Earth's Radiant Energy System (CERES).....	18
2.6.6 Lightning Imaging Sensor (LIS).....	19
2.7 TRMM Observation Principle	19

2.8	Data Products	21
2.9	COMB	22
2.10	Processing Algorithm.....	22
2.11	3B42 - TRMM Daily PRECIPITATION.....	22
2.12	ADVANTAGES OF SATELLITE PRECIPITATION DATA	23
2.13	USE OF SATELLITE DATA FOR FLOOD INUNDATION	24
2.14	Global Hydrologic Models	24
2.15	Modeling Approach	25
2.16	SWAT Hydrology	25
2.16.1	Surface Runoff	26
MATERIALS AND METHODS.....		28
3.1	ANALYTICAL FRAMEWORK.....	28
3.2	DATA COLLECTION	30
3.2.1	Topographic Data.....	30
3.2.2	Soil Data.....	31
3.2.3	Land Cover Data	32
3.2.4	In-situ Precipitation Data	33
3.2.5	Meteorological Data.....	34
3.2.6	In-situ River Discharge Data	34
3.2.7	Remote Sensing Precipitation Data	34
3.3	COMPARISON OF TRMM AND RAIN GAUGE DATA	35
3.4	STATISTICAL TEST	36
3.5	MODEL CALIBRATION	39
3.6	MODEL PERFORMANCE EVALUATION.....	39
RESULTS AND DISCUSSION.....		42
4.1	COMPARISON OF DAILY TRMM PRECIPITATION DATA AND PMD RAIN GAUGE DATA	42
4.1.1	Scatter Plots and Regression Analysis	42
4.2	COMPARISON OF MONTHLY TRMM PRECIPITATION DATA AND PMD RAIN GAUGE DATA	54
4.3	MODEL CALIBRATION AND VALIDATION.....	66
4.4	MODEL RUNOFF AND FLOOD INUNDATION MAPS	69
CONCLUSIONS AND RECOMENDATIONS.....		73
5.1	CONCLUSIONS.....	73
5.2	RECOMMENDATIONS FOR FURTHER RESESARCH.....	74
REFERENCES.....		75
APPENDICES		78

LIST OF FIGURES

Figure 1.1. Study area of Middle Indus River Basin is showing topography, major rivers, barrages and Pakistan Meteorological Department rain gauges in and around the study area.....	5
Figure 1.2. Mean annual rainfall variation over Pakistan from 1971-2000 is showing that the most of the country gets very small amount of rainfall per year and is therefore arid to semi-arid climate. Bulk amount of the rainfall is during monsoon season (July, August and September) and spring season (March, April and May) and is concentrated in the north quarter of the country. (Source: Pakistan Meteorological Department).....	5
Figure 2.1. Standard non- recording cylindrical rain gauge.....	9
Figure 2.2. A tipping bucket rain showing the bucket tips and cylinder.	9
Figure 2.3. Optical rain gauge.....	12
Figure 2.4. A wind shield placed around rain gauge to reduce wind effect.....	12
Figure 2.5. Tropical Rainfall Measuring Mission instruments PR, TMI, VIRS and LIS. ..	16
Figure 3.1.Flow diagram showing a step wise methodology adopted in this study.....	29
Figure 3.2. Daily stream flow hydrographs from 2003 to 2012 at Chashma and Guddu barrages in cumecs. The hydrographs of year 2003 and 2007, 2005 and 2006, 2008 and 2009, 2011and 2012 show similar pattern. (Source: FFC Islamabad, 2014).....	37
Figure 3.3. Methodology adopted for statistical analysis between TRMM daily precipitation data and in-situ PMD rain gauge data.	37
Figure 3.4. Manual calibration procedure for runoff calculation in SWAT model (modified after Santhi et al., 2001).	41
Figure 4.1. Scatter plots with regression line of daily TRMM versus PMD rain gauge data of 2003 showing maximum R^2 value 0.58 at Multan and minimum value 0.08 at Barkhan (n=365).	44

Figure 4.2. Scatter plots with regression line of daily TRMM versus PMD rain gauge data of 2005 showing maximum R^2 value 0.68 at Bahawalpur and minimum value 0.22 at D.G Khan (n=365).....	46
Figure 4.3. Scatter plots with regression line of daily TRMM versus PMD rain gauge data of 2008 showing maximum R^2 value 0.69 at Khanpur and minimum value 0.13 at Barkhan (n=366).	48
Figure 4.4. Scatter plots with regression line of daily TRMM versus PMD rain gauge data of 2010 showing maximum R^2 value 0.65 at D.G Khan and minimum value 0.22 at Mianwali (n=365).....	50
Figure 4.5. Scatter plots with regression line of daily TRMM versus PMD rain gauge data of 2012 showing maximum R^2 value 0.74 at Bahawalpur and minimum value 0.24 at Mianwali (n=366).....	52
Figure 4.6. Bar graphs of monthly TRMM versus rain gauge show the bimodal behavior in the area for year 2003.....	56
Figure 4.7. Bar graphs of monthly TRMM versus rain gauge show the bimodal behavior in the area for year 2005.....	58
Figure 4.8. Bar graphs of monthly TRMM versus rain gauge show the bimodal behavior in the area for year 2008.....	60
Figure 4.9. Bar graphs of monthly TRMM versus rain gauge show the bimodal behavior in the area for year 2010.....	62
Figure 4.10. Bar graphs of monthly TRMM versus rain gauge show the bimodal behavior in the area for year 2012.....	64
Figure 4.11. Calibration results of SWAT model on Middle Indus River basin from 2003 to 2010.....	68
Figure 4.12. Validation results of SWAT model on Middle Indus River basin from 2011-2012.....	68

Figure 4.13. Runoff generated by SWAT for 27th July 2010 precipitation..... 70

Figure 4.14. Runoff generated by SWAT for 28th July 2010 precipitation..... 70

Figure 4.15. Runoff generated by SWAT for 29th July 2010 precipitation..... 71

Figure 4.16. Runoff generated by SWAT for 8th September 2012 precipitation. 71

Figure 4.17. Runoff generated by SWAT for 9th September 2012 precipitation. 72

Figure 4.18. Runoff generated by SWAT for 10th September 2012 precipitation.. 72

LIST OF TABLE

Table 2.1. Table showing the main features of the Tropical Rainfall Measuring Mission satellite(Liu et al., 2013).	16
Table 2.2. Precipitation Radar System Parameters (Liu et al., 2013).	17
Table 2.3. TRMM Microwave Imager System Parameters (Liu et al., 2013).	18
Table 2.4. Visible and Infrared Scanner System Parameters (Liu et al., 2013).	18
Table 2.5. Clouds and the Earth's Radiant Energy System Parameters (Liu et al., 2013). ..	19
Table 2.6. Lightning Imaging Sensor System Parameters (Liu et al., 2013).	19
Table 2.7. TRMM data products provided by National Space Development Agency (Liu et al., 2013).	21
Table 3.1. Soil types with dominant soil, texture Class and texture in the study area.	32
Table 3.2. Land cover data with classes, codes and names.	33
Table 3.3. PMD Rain gauges with name, location (Latitude/Longitude) and elevation.	34
Table 4.1. Statistical results of year 2003 at PMD gauge stations in the area showing Correlation Coefficient, RMSE, Relative Bias and R^2 value (n=365).	43
Table 4.2. Statistical results of year 2005 at PMD gauge stations in the area showing Correlation Coefficient, RMSE, Relative Bias and R^2 value (n=365).	45
Table 4.3. Statistical results of year 2008 at PMD gauge stations in the area showing Correlation Coefficient, RMSE, Relative Bias and R^2 value (n=366).	47
Table 4.4. Statistical results of year 2010 at PMD gauge stations in the area showing Correlation Coefficient, RMSE, Relative Bias and R^2 value (n=365).	49
Table 4.5. Statistical results of year 2012 at PMD gauge stations in the area showing Correlation Coefficient, RMSE, Relative Bias and R^2 value (n=366).	51
Table 4.6. Five years daily average statistical results at all PMD gauge stations showing Correlation Coefficient, RMSE, Relative Bias and R^2 value.	53

Table 4.7. Monthly statistical results of year 2003 at PMD gauge stations in the area showing Correlation Coefficient, RMSE, Relative Bias and R^2 value (n=365).....	55
Table 4.8. Monthly statistical results of year 2005 at PMD gauge stations in the area showing Correlation Coefficient, RMSE, Relative Bias and R^2 value (n=365).....	57
Table 4.9. Monthly statistical results of year 2008 at PMD gauge stations in the area showing Correlation Coefficient, RMSE, Relative Bias and R^2 value (n=366).....	59
Table 4.10. Monthly statistical results of year 2010 at PMD gauge stations in the area showing Correlation Coefficient, RMSE, Relative Bias and R^2 value (n=365).....	61
Table 4.11. Monthly statistical results of year 2012 at PMD gauge stations in the area showing Correlation Coefficient, RMSE, Relative Bias and R^2 value (n=366).....	63
Table 4.12. Five years monthly average statistical results at PMD gauge stations in the area showing Correlation Coefficient, RMSE, Relative Bias and R^2 value.	65
Table 4.13. Default and adjusted ranges of SWAT model parameters used in calibration (Luzio et al., 2002).	66
Table 4.14. Model calibration and validation results with R^2 value, NSCE and Relative BIAS.....	69

LIST OF ABBREVIATIONS

Notation	Representation
ASCII	American Standard for Computer and Information Interchange
BIAS	Relative Bias
BIN	Binary
CC	Correlation Coefficient
CERES	Clouds and the Earth's Radiant Energy System
COMB	Combined
DEM	Digital Elevation Model
EOSDIS	Earth Observing System Data and Information System
ET	Evapotranspiration
FAO	Food And Agriculture Organization
FFC	Flood Forecasting Commission
GHz	Gaga Hertz
Ifov	Instantaneous Field of View
IGBP	International Geosphere Biosphere Programme
IIASA	International Institute for Applied System Analysis
LIS	Lightning Imaging Sensor
MODIS	Moderate Resolution Imaging Spectro-radiometer
MW	Microwave
NASA	National Aeronautics and Space Administration
NASDA	National Space Development Agency
NGA	National Geospatial-Intelligence Agency
NOAA	National Oceanic and Atmospheric Administration
PIA	Path Integrated Attenuation
PMD	Pakistan Meteorological Department
PPS	Precipitation Processing System
PR	Precipitation Radar
PRI	Pulse Repetition Interval
RMSE	Root Mean Square Error
RPM	Revolutions Per Minute
S/N	Signal to Noise
SCS	Soil Conservation Service
SRTM	Shuttle Radar Topography Mission
SSM/I	Special Sensor Microwave/Imager
SWAT	Soil and Water Assessment Tool
TMI	TRMM Microwave Imager
TRMM	Tropical Rainfall Measuring Mission
UNESCO	United Nations Educational, Scientific and Cultural Organization
USGS	United States Geological Survey
VIRS	Visible and Infrared Scanner
VIS/IR	Visible/Infrared

ABSTRACT

The impacts of floods and droughts are intensified by climate change, lack of preparedness and coordination. Pakistan lies in an arid and semi-arid climate zone with average rainfall ranging from less than 200 mm to more than 400 mm per year. In Pakistan rainfall is highly variable in its magnitude, time of occurrence and its spatial distribution. Rain gauge generally provides very accurate measurement of point rain rates and the amounts of rainfall but due to scarcity of the gauge locations provides very general information of the area on regional scale. Additionally, systematic and human errors make gauge data more prone to errors and mis-calculations. Recognizing these practical shortcomings of rain gauge data, it is essential to use remote sensing techniques for measuring the quantity of rainfall in the Middle Indus. This research uses satellite remote sensing of NASA's Tropical Rainfall Measuring Mission 3B42V7 estimates in terms of rainfall occurrence, quantity and its spatial distribution for Middle Indus Basin from Chashma barrage to Guddu barrage to model flood inundation. In order to use TRMM satellite data for flood inundation mapping, its accuracy is determined by statistically comparing it with in-situ gauged data on daily and monthly basis. Daily comparison results mention the average statistics with $CC= 0.64$, $RMSE= 4.69$, $Relative\ Bias\%= -14$ and $R^2= 0.42$ and monthly comparison with average $CC= 0.91$, $RMSE= 4.07$, $Relative\ Bias\%= 26$ and $R^2= 0.82$. The daily R^2 value is significantly lower than monthly R^2 value, probably due to the time of summation of TRMM 3-hourly precipitation data into daily estimates as opposed to the rain gauge data. It is also possible that the TRMM estimates fail to record the local development phenomena common in monsoon season. The in-situ rain gauge data

are generally recorded at about 0300 GMT, whereas TRMM daily estimates are the summed up from of 3-hourly collections from 0000 hours to 2100 hours GMT. Hence a difference of at least 6 hours is encountered in summing daily rain estimates. Daily TRMM data from 2003 to 2012 was used as input forcing in Soil and Water Assessment Tool (SWAT) hydrological model along with other input parameters like Land cover, temperature and soil data etc. The calibration and validation results of SWAT model give $R^2=0.72$ and 0.73 , NSCE= 0.69 and 0.65 respectively. Daily flood inundation maps are generated on the basis of model discharge output. The results of this research can be used by various stake holders, such as Pakistan Meteorological Department, Federal Flood Commission, Provincial Irrigation Departments and other planning and development authorities to investigate, plane, and analyze of climate change, floods, droughts and weather conditions.

INTRODUCTION

1.1 BACKGROUND

Rain is any product of water in the form of droplets that has condensed from atmospheric water vapor and then fall under the gravity. Rainfall is highly variable phenomenon spatially and temporally. Rainfall in Pakistan is also variable in its amount, time of occurrence and its distribution all over the country. The estimation of rainfall has been done by conventional rain gauges that sample the rain over a fixed time interval. The major shortcoming of this method is that the measurement is conducted only at selected points. The observations are fairly accurate at local scale. But it could not provide exact information on large scale. Satellite based precipitation has the advantage to provide spatially homogenous observations over large areas. Satellite measures the information of spatial distribution of rainfall and its quantity.

Generally; the trend of excess amount of rainfall is considered as a sign of flood and the shortage of rainfall is linked with drought in the area. Pakistan lies in an arid and semi-arid climate zone. In Pakistan rainfall period is highly variable because of its complex topography. Scarcely spaced rain gauges measure the rainfall over a fix time interval by quantifying the volume of rain water. Since there are a large number of rain gauges in Pakistan maintained by Pakistan Meteorological Department (PMD), but in middle Indus only a few rain gauges are available for measurement of rainfall in the area. These rain gauges can only provide general information of rainfall distribution on whole area. Recognizing the

practical limitations of rain gauges data, it is need of the hour to adopt remote sensing techniques for quantitative measurement of rainfall in Pakistan and especially in Middle Indus.

At present, with the advancement of sophisticated satellite technology, research on rainfall can be done by using satellite estimated data from weather satellites. Weather satellites have been particularly intended for the observation and estimation of the structure and vaporous segments of the Earth's environment as well as climatic phenomena, like, rainfall, cloud formation, wind and tropical storm generation. Remote sensing techniques are being employed to measure precipitation since late 1970s. Active and passive sensors are used in remote sensing based precipitation estimates. Passive sensors are manufactured to detect the reflected solar energy by rain droplets or clouds. The brightness characteristics of the cloud in visible images and temperature characteristics of the clouds in infrared images provide the initial precipitation estimates from the satellite data.

The Tropical Rainfall Measuring Mission (TRMM 3B42V7) satellite data has been used in this study to measure the abilities of TRMM satellite in accessing the amount of rainfall and its spatial distribution in the study area. This study involves data collection and comparison of satellite estimates and in-situ rain gauge data between Chashma and Guddu barrage over a period of ten years (2003-2012). The daily satellite TRMM 3B42V7 precipitation data has been compared statistically with in-situ rain gauge data in order to analyze its accuracy. Then by using this satellite TRMM 3B42V7 precipitation data flood inundation maps has been generated using SWAT hydrological model.

1.2 RATIONALE

In vicinity of the study area there are about eight rain gauges maintained by PMD, satellite Rain estimation will be employed to overcome the in-situ data scarcity in the study area. By using the application of remote sensing based on satellite data as a medium in processing of rainfall distribution, it will help to overcome the deficiency of rain gauge network stations. In addition, it can contribute to the field of study in order to find the most effective precipitation data from other satellites. Satellite derived precipitation products, such as TRMM 3B42V7 should be used as input into hydrological models for the purposes of generating runoff estimates and river discharge values. By knowing the accuracy of satellite data, it can help meteorological department in their investigating of predicted climate change, floods, droughts and weather condition.

1.3 OBJECTIVES

The aim of this research is to compare the effectiveness of satellite TRMM daily data for rainfall distribution to generate flood inundation maps of middle Indus river basin from Chashma to Guddu barrage. Based on the general aim above, following objectives are carried out to achieve the main aim of this research:

1. To compare and validate spatial distribution of precipitation TRMM daily data with in-situ rain gauge daily data.
2. To apply SWAT model to Middle Indus basin between Chashma and Guddu barrage.
3. To generate flood inundation maps on the basis of model discharge.

1.4 STUDY AREA

This research was conducted on Middle Indus River Basin from Chashma to Guddu barrage. The study area falls in the administrative districts of Dera Ismail Khan, Bhakkar, Layyah, Dera Ghazi Khan, Muzaffargrah, Rajanpur and Rahim Yar Khan. The extent of the watershed stretches from 27°-34°N and 69°-74°E. The watershed has an area of about 204,525 square kilometers (Figure 1.1).

1.5 CLIMATE

The climate of Pakistan varies from tropical to temperate zone, just above the tropic of cancer. On the basis of temperature, there are five regions (hot, warm, mild, cool, and cold). Four climatic regions have been identified in Pakistan (1) Arid, (b) Semi-arid, (c) Sub-humid, and (4) Humid. The southern parts of the country have high temperature that decreases toward north (Khan et al., 2010).

1.6 RAINFALL

In Pakistan rainfall is highly variable spatially and temporally. There are four rainy seasons (1) winter rainfall, (2) pre-monsoon rainfall, (3) monsoon rainfall (4) post monsoon rainfall. On the basis of amount of rainfall the two seasons winter and monsoon are called as moistest seasons while the other two are considered as the driest seasons in the country. The Figure 1.2 shows mean annual rainfall over Pakistan from 1971-2000. This figure clearly represents the spatial distribution of rainfall and shows that most of the rainfall in northern parts of the country. This figure also describes the study area has average 200mm to 600mm rainfall per year.

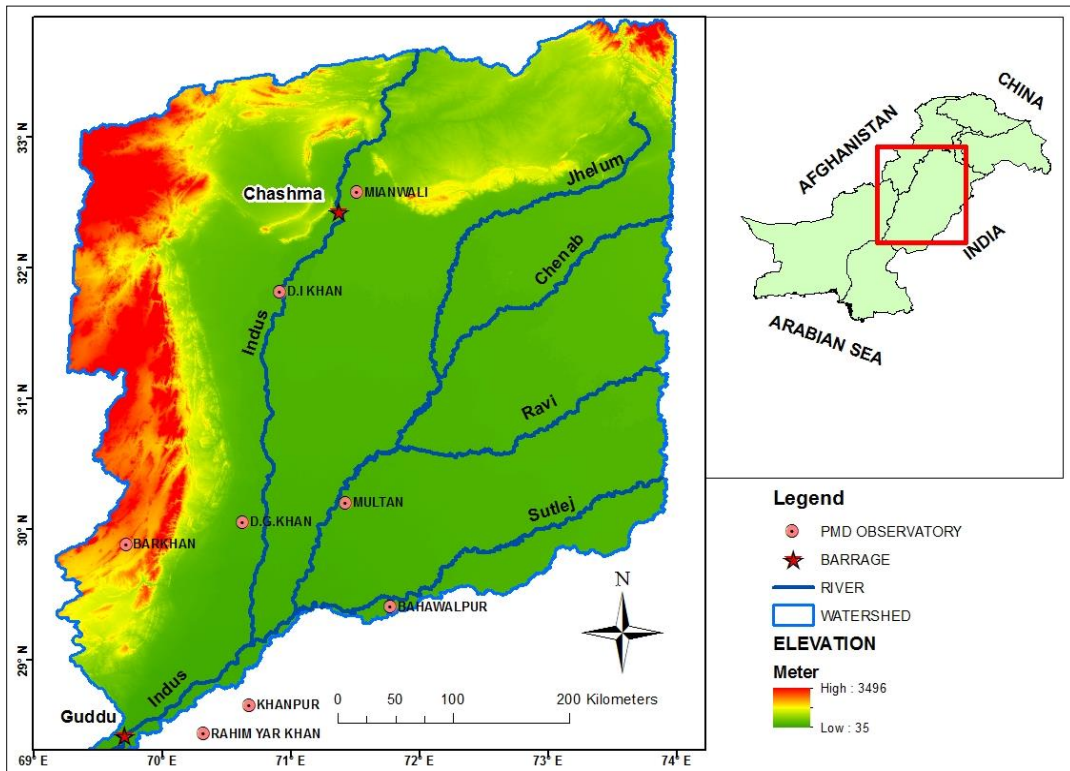


Figure 1.1. Study area of Middle Indus River Basin is showing topography, major rivers, barrages and Pakistan Meteorological Department rain gauges in and around the study area.

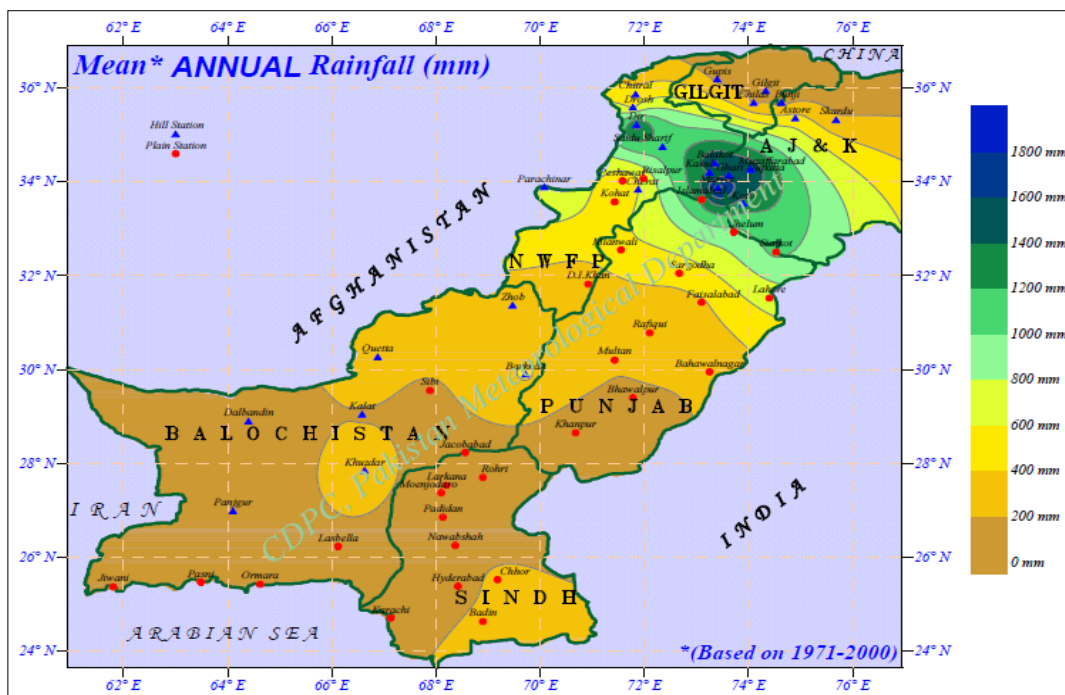


Figure 1.2. Mean annual rainfall variation over Pakistan from 1971-2000 is showing that the most of the country gets very small amount of rainfall per year and is therefore arid to semi-arid climate. Bulk amount of the rainfall is during monsoon season (July, August and September) and spring season (March, April and May) and is concentrated in the north quarter of the country. (Source: Pakistan Meteorological Department)

The heavy rainfall receives during summer is due to southwesterly winds called monsoon whereas high rainfall in winter is because of southwesterly winds called western disturbances. The northern parts of the country receive heavy rain thunderstorms which are caused by convectional air uplifting due to local heating (Khan et al., 2010).

1.7 HYDROLOGY

River Indus is the largest river of Pakistan which flows from Tibet (China) in central Himalayas, westward through Kohistan and Karakoram and then southward through Punjab plains to flow into Arabian Sea south of Kotri. Indus is divided into two parts, the Upper Indus that starts from extreme north of Pakistan and ends up to Mithankot and the Lower Indus from Mithankot up to Thatta. River Indus flows from north to south and has its tributaries on both western and eastern sides. The western side tributaries are Swat, Kabul, Kurram, Tochi, Gomal and Zhob rivers. The eastern side tributaries are Jehlum, Chennab, Ravi and Sutlej rivers. These four eastern side rivers meet Indus River at a location known as Pajnad which means five rivers in local language. From here downstream, Indus River flows alone through the lower Indus plain, eventually flowing into the Arabian Sea to feed Indus delta.

1.8 AGRICULTURE

Pakistan is known as an agricultural country all over the world and its most important crops are wheat, cotton, rice, corn and sugarcane, which altogether account for more than 75% of the total crop output of the country. In Pakistan, more than 95% of country's water resources consumption is in agriculture use and the remaining amount of water is used for household purposes (Bhatti et al., 2009).

Although the use of underground waters is increasing, Pakistan is solely dependent on the waters from the Indus river system and its tributaries.

1.9 SCOPE OF THE STUDY

The main aim of this study is to evaluate the hydrological response of the Middle Indus River Basin to satellite and in-situ rain gauge estimates using SWAT hydrological model. The hydrological response will be characterized by satellite based forcing of precipitation and in-situ Evapotranspiration (ET) and infiltration in a relatively un-gauged stretch of the Indus River Basin from Chasmha to Guddu.

CHAPTER 2

REVIEW OF LITRATURE

2.1 PRECIPITATION AND ITS MEASUREMENT

Precipitation is any product of the condensed atmospheric water vapor that falls under gravity. Rain gauges are simple instrument that are made to estimate the quantity of precipitation that comes to the surface during a rainfall. In history rainfall has been measured using conventional rain gauges which provide the amount of rainfall and its depth at a point. The general rule of measuring rainfall using rain gauges is to accumulate rain water in a fixed diameter cylinder and measure the volume of water in units of height (inches or millimeters). This total volume of collected water is divided by the opening of the cylinder area and then converted into amount of rainfall. (" Glossary of Meteorology" 2014).

2.2 RAIN GAUGES TYPES

There are different types of rain gauges that are categorized into two main classes:

2.2.1. Non-Recording Gauge

Non-recording gauge is a basic water storage device that measures the accumulated water of rainfall. The standard rain gauge is simple large cylinder with a funnel and a plastic tube for measurement as shown in Figure 2.1.



Figure 2.1. Standard non- recording cylindrical rain gauge.



Figure 2.2. A tipping bucket rain showing the bucket tips and cylinder.

(Source: <http://novalynx.com/products/rain-gauges/260-2500-tipping-bucket-rain-gauge>)

2.2.2. Recording Gauges

Recording rain gauges are manufactured to measure the amount of rainfall that reaches the ground during an event automatically. There are different types of recording gauges:

- Tipping bucket rain gauge
- Weighing rain gauge
- Telemetric rain gauge

2.2.2.1 Tipping bucket rain gauge

These rain gauges consist of a cylinder (usually 8 or 12 inch diameter) with a pair of buckets that are placed in horizontal axis (Figure 2.2). When a fixed quantity of rainfall water is collected into the buckets, nearly 0.01 inches the bucket tips to the other bucket that collects the next rain water. In each tip, an electronic signal is sent to data logger which is connected to computer. By counting the known amount of tips and their re-occurrence times make easy to calculate the amount of precipitation. This method can also be used to measure the rate of rainfall change during an event.

2.2.2.2 Weighing rain gauge

The weighing rain gauge works on the principle of weighing the amount of rainfall water that is collected in the buckets. The rainfall rate is calculated by the difference in rainwater that is accumulated in the gauge over a given time interval. The accuracy of the calculated rain rate which is directly related to the precision of the water accumulation measurement and the sampling interval (Nuystuen, 1999).

2.2.2.3 Optical rain gauge

The optical rain gauges measure the intensity of infrared light that falls on water droplets between a light source and a receiver (Nystuen et al., 1996). The change of intensity of light on receiver is caused due to droplet size, velocity, shape and the light source (Liu et al., 2013). These rain gauges are comparatively more sensitive, accurate and expensive. These gauges are usually used for research purposes (Figure 2.3).

2.3 ERROR IN RAIN GAUGE MEASUREMENT

The rain gauges are the most simple and direct instruments for measuring amount of precipitation and its depths, but they are affected by many sources of errors and uncertainties. The major sources of errors are due to wind and temperature effects which are:

2.3.1 Wind-Induced Errors

The rain gauges are mostly placed few feet above the ground, it is done so as to avoid wind eddies which are formed around their vents causes a reduction to catch small rain drops. This is the most common and serious source of error known as wind-induced gauge under-catch. This error can be minimized by placing wind protecting shields around the rain gauges as shown in Figure 2.4.



Figure 2.3. Optical rain gauge.



Figure 2.4. A wind shield placed around rain gauge to reduce wind effect.

(Source: <http://novalynx.com/products/rain-gauges/260-952-alter-type-rain-gauge-wind-screen/>)

2.3.2 Evaporation and Wetting Loss

Evaporation and wetting loss is experienced in non-recording rain gauges, when recording is done after a long time interval. These losses depend upon temperature, relative humidity, the time between rain events and the accumulation of the rain.

2.3.3 Calibration Errors

Calibration error usually occurs in tipping-bucket rain gauges. These gauges need some calibration and adjustment at a fixed small or intermediate rain event on the tipping mechanism (generally referred to as static calibration).

2.3.4 Other errors in rain gauge measurements

Additional sources of error in rain gauge measurements include splashing of precipitation, electronic and mechanical breakage of the rain gauges, clogging of rain gauge vents and funnels, observer mistakes in reading, processing and distribution of rainfall estimates. The configuration and installation of rain gauges close to trees or buildings can cause large errors. There is a general rule that an obstruction object should be as far as twice the object height above the ground.

2.4 SATELLITE BASED PRECIPITATION ESTIMATES

Perceiving the practical shortcomings of rain gauge, researchers have progressively attracted to remote sensing for quantifying the precipitation over the regional scale. In any case, remote sensing will be utilized as a supplement not the substitution of conventional traditional method for precipitation estimation. The measurement of precipitation by using rain gauges is full of undesirable errors but is relatively simple and cheap method to provide the rainfall data. Satellite based

precipitation technique provides extended precipitation coverage beyond ground in situ gauged data. Satellite data provides continuous temporal and spatial countrywide coverage of rainfall especially over complex terrain and un-gauged regions that lacks sufficient surface based observations.

Satellite Precipitation estimate was quantitatively evaluated over Middle Indus basin, located within the TRMM product latitude band ranging from 27°-34°N. The TRMM version of 3B42V7 precipitation data set is used to assess the precipitation variability. TRMM product has shown varying accuracies in different regions and for different adopted methods. Ji and Stocker (2003) and Chongamwong et al. (2006) observed correlation of 0.56 and 0.86 between satellite and rain gauge measurements, respectively. This product is quantitatively evaluated against measurements from rain gauges middle Indus basin in Pakistan.

2.5 OVERVIEW OF SATELLITE PRECIPITATION DATA

The environmental change has turned into a regional problem in recent decade. Satellite remote sensing is an essential and powerful means of estimating the worldwide environmental change (Center, 2001). In spite of this global rainfall coverage estimation, it is extremely difficult to exact measurement of rainfall because rain is a high spatial and temporal variable. Therefore satellite remote sensing has also some limitations and problems in estimation of rainfall. But it is the only method to provide near real time rainfall data on regional scale. TRMM with first space borne rain radar satellite is the first space mission used to measure and monitor rainfall over tropical and subtropical regions using microwave and visible/infrared sensors.

2.6 TROPICAL RAINFALL MEASURING MISSION

2.6.1 Introduction

TRMM satellite was launched at November 28, 1997 by Space Center of National Space Development Agency of Japan (NASDA). This satellite was a joint project between Japan and United States. TRMM is the first space project that is designed to measure precipitation. TRMM satellite basically observes rain structure and rainfall spatial distribution in tropical and subtropical regions. This satellite precipitation data was expected to play a vital role for understanding the regional and global climate change monitoring.

The TRMM observatory has five instruments, (1) Precipitation Radar (PR), (2) TRMM Microwave Imager (TMI), (3) Visible and Infrared Scanner (VIRS), (4) Clouds and the Earth's Radiant Energy System (CERES) and (5) Lightning Imaging Sensor (LIS) as shown in Figure 2.5. TRMM precipitation measurement has three instruments (PR, TMI, and VIRS) to measure precipitation of tropical and subtropical regions. The main features TRMM are described in Table 2.1.

2.6.2 Precipitation Radar (PR)

The Precipitation Radar (PR) is a primary instrument that is installed on TRMM. The PR is the first most recent of the five TRMM instruments for quantitative measurement of rain. The major objectives of PR are:

- (a) To provide a three dimensional precipitation structure.
- (b) To measure quantitative estimation of the precipitation over land and ocean.

Table 2.1. Table showing the main features of the Tropical Rainfall Measuring Mission satellite (Liu et al., 2013).

Launch weight	Approximate 3.62 ton
Launcher	H-II Rocket
Launch date	November 28, 1997
Altitude	350 km (1997/11/27 - 2001/08/08) 403 km (2001/08/24 - present)
Inclination	Approx. 35 degrees
Power	~ 1100 W
Design life	3 years and 2 months
Instruments	Precipitation Radar (PR) TRMM Microwave Imager (TMI) Visible and Infrared Scanner (VIRS) Clouds and the Earth's Radiant Energy System (CERES) Lightning Imaging Sensor (LIS)

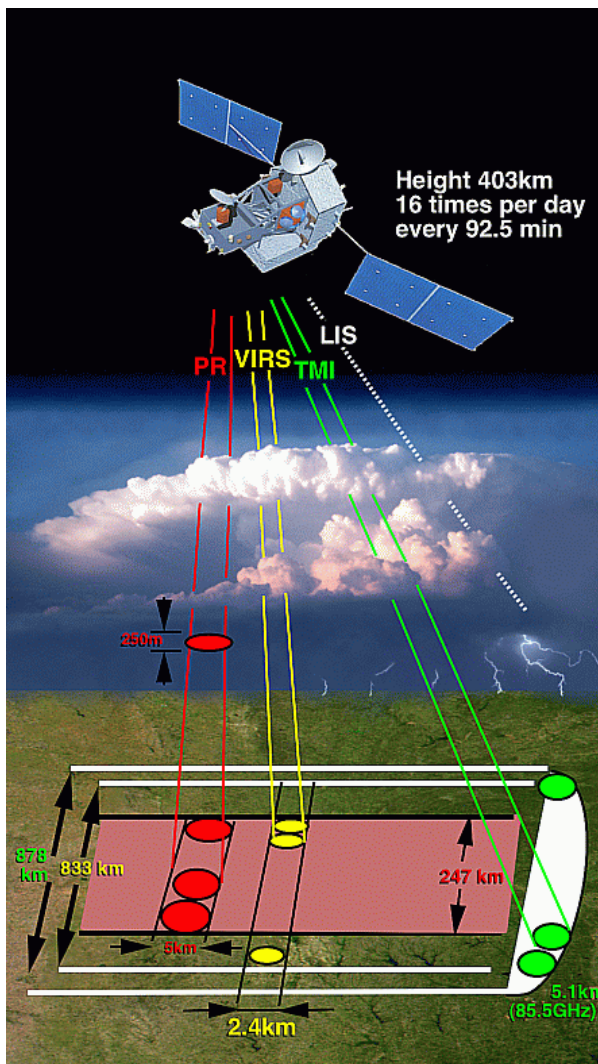


Figure 2.5. Tropical Rainfall Measuring Mission instruments PR, TMI, VIRS and LIS.

The PR data is instrumental to obtain the precipitation height profile when combined it with TMI. For small rainfall measurement ground based radar algorithm is applied for rainfall estimation. For heavy rainfall measurement, a attenuation rain correction factor is used. The parameters of PR are described in Table 2.2.

Table 2.2. Precipitation Radar System Parameters (Liu et al., 2013).

Radar Type	Active Phased array Radar
Frequency	13.796 GHz and 13.802 GHz
Swath Width	~ 215 km
Range Resolution	250 meter
Horizontal Resolution	4.3 ± 0.12 km (at Nadir)
Weight	465 kg
Power	213 W

2.6.3 TRMM Microwave Imager (TMI)

The TRMM Microwave Imager is a dual-polarized instrument with Multi-channel passive microwave radiometer. It uses nine channels having frequencies of 10.65 GHz, 19.35 GHz, 21.3 GHz, 37 GHz, and 85.5 GHz. The TMI instrument provides accurate data of precipitation over the sea, but relatively less reliable precipitation data over land because of non-homogeneous surface emissions. The parameters of TMI sensor are described in Table 2.3. The TMI data can also be utilized for measurement of precipitation profiles by combining it with the PR and VIRS data (Liu et al., 2013).

Table 2.3. TRMM Microwave Imager System Parameters (Liu et al., 2013).

Observation Frequency	10.65, 19.35, 21.3, 37 and 85.5 GHz
Horizontal Resolution	06-50 km
Swath Width	~ 760 km
Scan Mode	Conical Scan (490)
Weight	50 kg
Power	39 W

2.6.4 Visible and Infrared Scanner (VIRS)

The Visible and Infrared Scanner instrument is radiometer that scans cross-track operating in the visible to infrared spectral regions in five spectral bands. VIRS is similar to the instruments which were launched on other meteorological satellites. The VIRS data is used in the estimation of precipitation algorithms which are based on satellite active and passive microwave sensors. The parameters of VIRS sensor are described in Table 2.4.

Table 2.4. Visible and Infrared Scanner System Parameters (Liu et al., 2013).

Swath Width	Scan angle \pm 450, 720 km at ground
Scan Angle	3600
Rotation Rate	98.4 rpm
IFOV	6.02 mrad 2.11 km (nadir)
Weight	49 kg
Power	53 W

2.6.5 Clouds and the Earth's Radiant Energy System (CERES)

The CERES instrument is helpful instrument to reduce the major errors and uncertainties in long term climate changes prediction. The top of the Earth's atmosphere radiant fluxes are measured by using the Earth Radiation Budget Experiment. It can easily differentiate the change between fluxes generated from clear sky and cloudy atmospheres. The CERES algorithm can provide a better understanding of cloud convective processes, the effect of top Earth's fluxes and boundary layer meteorology. CERES can also be used to evaluate the surface

radiation budget that is essential in study of atmospheric energy, biological productivity and transfer of air-sea energy. The parameters of CERES sensor are described in Table 2.5.

Table 2.5. Clouds and the Earth's Radiant Energy System Parameters (Liu et al., 2013).

Observation Band	0.3 – 5 μm (short Wave Channel) 8 – 12 μm (Long Wave Channel) 0.3 ~> 50 μm (Total Wave Channel)
Horizontal Resolution	10km
Swath Width	Scan Angle \pm 820
Scan Mode	Cross-Track Scan or Biaxial Scan
Weight	45.5 kg
Power	47 W

2.6.6 Lightning Imaging Sensor (LIS)

The Lightning Imaging Sensor (LIS) is a filter imaging system with optical telescope. It has capability to acquire and examine the variability and distribution of intra-cloud lightning and cloud-to-ground lightning in the atmosphere. LIS data can also be used along with PR, TMI and VIRS to measure the relationships of regional rainfall occurrence and other storm properties. The LIS data can be linearly related to regional rainfall, depths, spatial distribution and movement of latent heat. The parameters of LIS sensor are described in Table 2.6.

Table 2.6. Lightning Imaging Sensor System Parameters (Liu et al., 2013).

Observation Band	0.777655 μm
Horizontal Resolution	4 km
Swath Width	~ 600 km
Weight	18 kg
Power	42 W

2.7 TRMM OBSERVATION PRINCIPLE

The major principle of TRMM precipitation estimations using satellite radar is to use the radio waves. The radio waves are emitted from radar; they are reflected by the rain droplets in the atmosphere and a part of these waves reflect

back to the radar receiver (backscattering). The amount of precipitation measurement is based on the relation between the intensity of scattered radio waves and rainfall intensity received by the radar receiver. In the radar equation some conditions are adjusted such as, the diameter of the rain droplets are very small to the wavelength of the radio wave (< 5 m), rain droplets are equally distributed in the radar beam and with constant the speed (Liu et al., 2013).

The precipitation radar sends two frequencies pulse waves (F1 = 13.796 GHz, F2 = 13.802 GHz) after each 360.23 μ sec, this is called transmission of pulse repetition interval (PRI) time. Radar sends a single beam in 32 pulses from an orbital altitude of 403 km. Radar measures the received power strength of the returned radio waves. Total sixty four pulses (32 x 2 frequencies) data are averaged and sent to the ground. The PR scans cross track direction of the satellite after every 0.6 seconds. The PR has 49 beams with a beam at 0.71 degrees within the range of ± 17 degrees with the center at nadir. Every scan is the output of 49 observations to beam directions. The precipitation radar is active phased array system radar which has a transmitter and a receiver connected to on board TRMM. The precipitation radar is manufactured so that correct information can be obtained at the satellite altitude range 403 km + 7 km and - 8 km. The received data may be missing, or ground surface echo may not be included in the observation data outside this range (Liu et al., 2013).

The observation of precipitation using radar from space differs from on ground radar precipitation because space radar has a strong scattering echo than from the ground radar. This rainfall attenuation echo is used to improve the estimated rainfall intensity accuracy. The precipitation radar data is sampled for a

range of resolution (250 m). This processing is done by the algorithm installed in the system control and data processing unit.

2.8 DATA PRODUCTS

National Space Development Agency of Japan (NASDA) provides the following TRMM data products as described in Table 2.7.

Table 2.7. TRMM data products provided by National Space Development Agency (Liu et al., 2013).

Sensor	Processing Level	Product	Scene Unit	Estimated Data Volume
PR	1B21	Calibrated Received Power	1 orbit (16/day)	149 MB (60~70 MB)
	1C21	Radar Reflectivity	1 orbit (16/day)	149 MB (40~50 MB)
	2A21	Normalized Radar Surface Cross Section (s^0)	1 orbit (16/day)	10 MB (6~7 MB)
	2A23	PR Qualitative	1 orbit (16/day)	13 MB (6~7 MB)
	2A25	Rain Profile	1 orbit (16/day)	241 MB (13~17 MB)
	3A25	Monthly Statistics of Rain Parameter	Global Map (Monthly) (Grid: $5^\circ \times 5^\circ$, $0.5^\circ \times 0.5^\circ$)	40 MB (26~27 MB)
	3A26	Monthly Rain Rate using a Statistical Method	Global Map (Monthly) (Grid: $5^\circ \times 5^\circ$)	9.3 MB (5~6 MB)
TMI	1B11	Brightness Temperature	1 orbit (16/day)	14 MB (14 MB)
	2A12	Rain Profile	1 orbit (16/day)	97 MB (6.7~9 MB)
	3A11	Monthly Oceanic Rainfall	Global Map (Monthly) (Grid: $5^\circ \times 5^\circ$)	53 KB (44 KB)
VIRS	1B01	Radiance	1 orbit (16/day)	92 MB (90 MB)
COMB	2B31	Rain Profile	1 orbit (16/day)	151 MB (8 MB)
	3B31	Monthly Rainfall	Global Map (Monthly) (Grid: $5^\circ \times 5^\circ$)	442 KB (380~410 KB)
	3B42	TRMM & IR Daily Rainfall	Global Map (Daily) (Grid: $0.25^\circ \times 0.25^\circ$)	242 KB (110~115 KB)
	3B43	TRMM & Other Sources Monthly Rainfall	Global Map (Monthly) (Grid: $1^\circ \times 1^\circ$)	242 KB (242 KB)

2.9 COMB

COMB is the combined data products of PR and TMI products. COMB rain dataset consists of corrected correlation mass-weighted, mean drop diameter, coefficient of rain rate attenuation and Path Integrated Attenuation (PIA). Standard deviation is also calculated of each COMB parameter (Liu et al., 2013).

2.10 PROCESSING ALGORITHM

The main aim of 3B42 data set is to provide a precipitation estimates that have approximate zero biasing of the "TRMM Combined Instrument" precipitation. It has a thick sampling procedure of geo-synchronous Infrared imagery. For 3B42 processing, the intermediate product of TMI, 3B31, 3A46 and 3A45 are used as input data. TRMM 3B42 data is consisted of two following objectives:

- (1) To produce monthly based IR calibration parameters.
- (2) To calibrate the merged-IR precipitation data to produce the daily estimated precipitation and the Root Mean Square Error measurements.

2.11 3B42 - TRMM DAILY PRECIPITATION

The 3B42 V7 daily precipitation data is grid based data with resolution of (0.25°x0.25°) grid structure. Describing 3B42 TRMM daily precipitation format, the following parameters are used:

nlat = 80: The number of 0.25° grid intervals of latitude from 40° N to 40° S.

nlon = 360: The number of 0.25° grid intervals of longitude from 180°W to 180°E (Center, 2001).

2.12 ADVANTAGES OF SATELLITE PRECIPITATION DATA

Satellite precipitation data have a lot of advantages, being an efficient and cost effective data for large areas, have a continuous near global coverage over a large period of time. Satellite rainfall observations have introduced in the past decade as a valuable data source for a large extent of hydrological applications at global scale. It includes flood extent maps and weather forecasting (Artan et al., 2007), water management, hydrological processes; and landslide susceptibility and prediction (Hong et al., 2007).

In previous research, satellite rainfall data were validated using ground rainfall data (Ohsaki et al., 1999). In general, the satellite rainfall estimation data validation research has found that the accuracy can be influenced by many factors such as geographical location, climate, time period and rainfall type (Nicholson et al., 2003).

A study of satellite rainfall data accuracy was archived by Islam and Uyeda (2008). They have analyzed different satellite precipitation data sources TRMM 3B42 V5, 3B43 V6 and Bangladesh Meteorological Department in-situ rain gauges network during pre-monsoon to post-monsoon periods in Bangladesh. They concluded after comparing satellite data with rain gauges data that satellite rainfall data is overestimated in arid regions and during the pre-monsoon season, but underestimated in humid regions and during the monsoon season.

The precision and accuracy of the satellite precipitation data can be different for different geographic or climatic regions. Rapidly increased urban areas can be new factors affecting the accuracy of satellite rainfall data, because climatic characteristics are changed by the urbanization (Sharma et al., 2007).

According to previous research, satellite rainfall data provide reasonable estimated rainfall data. However, the validation of accuracy for satellite rainfall data is lacking in urban areas, which is one of the most important places for water management and flood control because of dense population areas.

2.13 USE OF SATELLITE DATA FOR FLOOD INUNDATION

The satellite precipitation data provides a conservative, useful and cost effective rainfall data and amount over large areas. The use of satellite precipitation data in global hydrological studies and modeling remains limited because the satellite data accuracy always remains a question. The datasets are large and very cumbersome to use in modeling, and the impact on hydrologic model errors is also uncertain. There have been specific questions raised about the accuracy of satellite rainfall data, how this data is validated for use and how it is effected by topographical characteristics, in terms of time, rainfall pattern and cloud types (Artan et al., 2007).

2.14 GLOBAL HYDROLOGIC MODELS

Regional-to-global scale hydrologic and flood modeling is an essential tool needed to plan for water supply management and flood control (Hossain & Katiyar, 2006). Based on the increased interest of global scale studies, several global hydrologic models have been developed (Vorosmarty et al., 1989). The development of the global hydrologic model has presented many difficulties such as the complexity of the hydrological processes, the regional scale monitoring and the low quality of the input datasets. Spatial resolution is especially important for global scale hydrologic models.

2.15 MODELING APPROACH

A first attempt at global runoff modeling using global satellite precipitation data was introduced by (Hong et al., 2007). He presented a global runoff model applying the well-known SCS CN method. The model result is a daily-based 1 km spatial resolution runoff response, because the finest spatial resolution data is land use and it has 1 km spatial resolution. In this research Soil and Water Assessment Tool (SWAT) Hydrological model is used. SWAT is a physical based semi distributed basin scale model. It is a continuous simulated model that operates on daily and monthly time steps. It is designed to estimate the impacts of management on water, sediments flow and agricultural chemical yields in the area. This model is capable of predicting water quantity, water quality and sediment yields from a large, complex watersheds having variable land cover, slop and soil types (Tech, 2013). SWAT model simulates surface runoff, sediments flow and nutrients yield, pesticide, bacteria effects on crop yields (Arnold et al., 1995). This model divides sub- watersheds into further small units called hydrological response units (HRUs). The hydrologic response unit (HRUs) consists of same type of land cover, soil characteristics and management practices (Gassman et al., 2007). Further sub-division of sub-basins into HRUs enables to account the impact of different land cover types, management practices and soil characteristics on the hydrologic cycle of the basin.

2.16 SWAT HYDROLOGY

Similar to most river basin models, SWAT model runs the water balance equation for a river basin. The two modules are used in the simulation of any basin hydrology:

- (i) The land phase that controls the amount of soil moisture and nutrient concentration at each HRUs and sub-basin.
- (ii) The routing phase which deals with the transfer of water and sediments through the stream networks of the basin.

The water balance equation used and run in SWAT model which represent the hydrologic cycle can be expressed as:

$$SW_t = SW_0 + \sum_{i=1}^t (P - Q_f - ET_a - W - Q_g)$$

Where

SW_t = Soil water content at time (mm)

SW_0 = Initial soil water contents (mm)

t = Time (days)

P = The amount of rainfall (mm)

Q_f = Surface runoff (mm)

ET_a = Evapotranspiration (mm)

W = Water entering in the vadose zone from the soil (mm)

Q_g = Return flow (mm)

2.16.1 Surface Runoff

When water is applied to the field, it starts in infiltrating in the soil depleting the moisture deficit in the soil. When application rate is greater than the infiltration rate, depression storage starts at the surface. Once the depression storage completed, water start moving in the direction from higher to lower elevation. This surface movement of water is considered as surface runoff. SWAT

uses Soil Conservation Services (SCS) curve number method to estimate the surface runoff calculation (Neitsch et al., 2005). SCS curve number is an empirical method used in model which shows relationship between runoff and rainfall that gives an estimation of the amount of runoff for different land cover and soil types.

The equation of SCS curve number is mathematically shown as:

$$Q_f = \frac{(R_d - I_i)^2}{(R_d - I_i + S)}$$

Where

Q_f = Runoff or rainfall excess (mm)

R_d = Rainfall on a given day (mm)

I_i = Interception and infiltration (mm)

S = Surface Retention (mm)

Surface Retention S varies spatially and depends upon soil type, land cover and management practices. Mathematically it is expressed as:

$$S = 25.4 \left(\frac{100}{CN} - 10 \right)$$

Where:

CN = Curve number.

MATERIALS AND METHODS

This chapter discusses the study area of middle Indus river basin from Chashma to Guddu barrage briefly and the overall methodology that has been adopted in this research. In hydrologic models generally precipitation is the major forcing agent of simulation of stream flows and storm runoff. First of all the satellite based precipitation estimation of Tropical Rainfall Measuring Mission (TRMM) were statistically compared with Pakistan Meteorological Department (PMD) rain gauge daily data, in order to develop confidence in TRMM dataset. In this research Soil Water Assessment Tool model is selected to conduct simulations of storm and stream runoff.

3.1 ANALYTICAL FRAMEWORK

The flow chart is showing the overall methodology adopted in this research as in Figure 3.1. The step by step procedure used for the simulation of the SWAT model, calibration and validation processes are:

- Data Collection
- Data Pre-processing
- Sensitivity Analysis
- Model Calibration and Validation
- Analysis

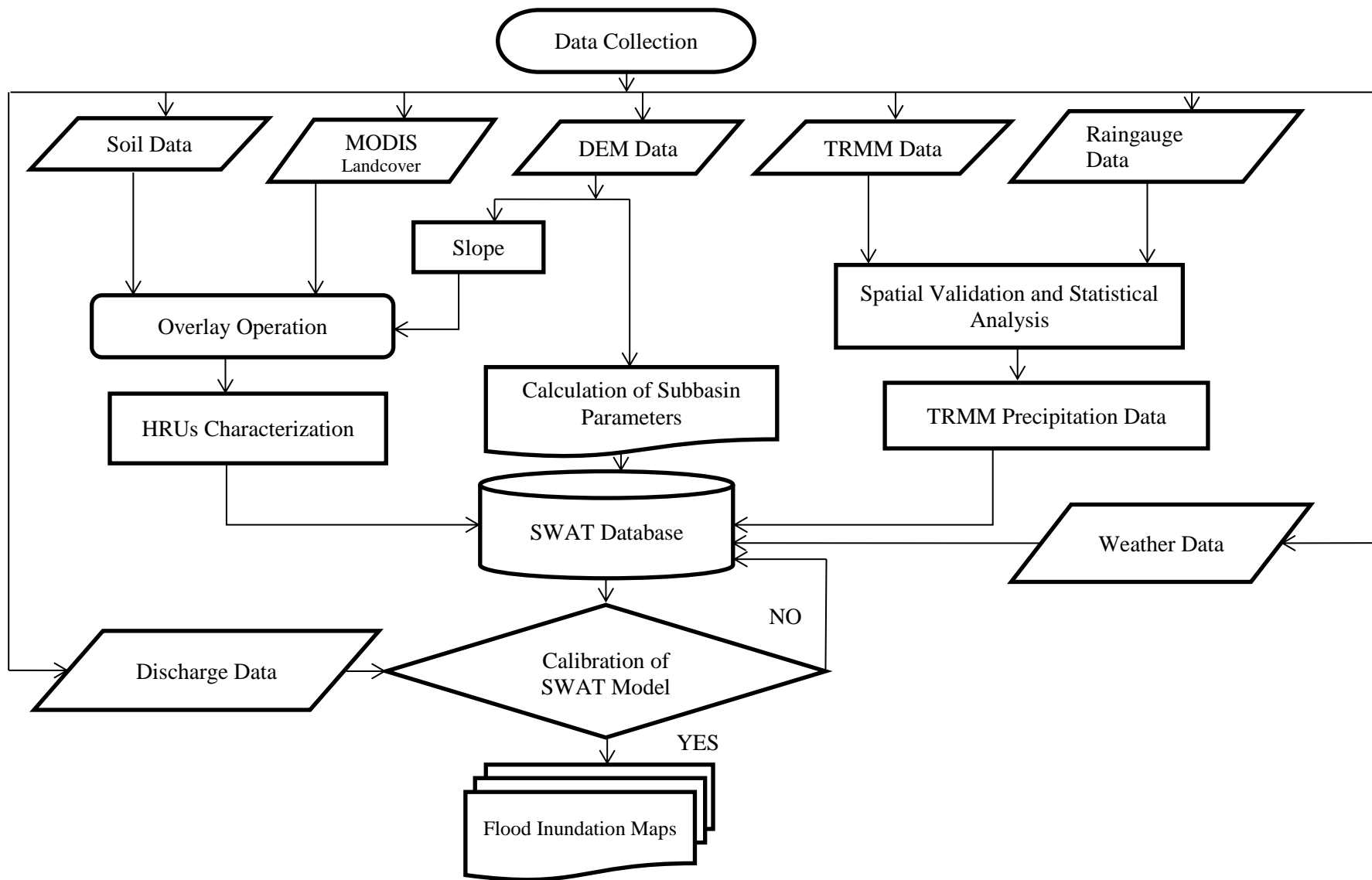


Figure 3.1. Flow diagram showing a step wise methodology adopted in this study

3.2 DATA COLLECTION

The datasets used in this research are described below:

- Topographic data
- Soil data
- Land cover data
- In-situ precipitation data
- Meteorological data
- In-situ river discharge data
- Remote sensing (TRMM) precipitation data

3.2.1 Topographic Data

Topographic data was extracted from remotely sensed data acquired by NASA and is freely available on internet as Digital Elevation Model (DEM) data files. The digital elevation model contains the ground elevation values from a referenced fixed datum; it is usually generated at regular intervals and fixed grid space. The DEM is a basic and most important source of information for the other models which are dependent on elevation. Hence, the quality of the model is dependent on the quality and resolution of the DEM used. Most of the DEMs include certain odd grid cells (i.e. areas) with special characteristics which require different symbology. These areas/grid cells represent minor imperfections in the topography and counted as errors in many software programs. These errors need to be found and correction is made before the DEM used.

One of the most popular DEM, freely available for near global coverage, at 90 meters horizontal spatial resolution was acquired using radar sensor aboard

space shuttle in year 2000 is Shuttle Radar Topography Mission (SRTM). SRTM is an international joint project between US National Aeronautics and Space Administration and the National Geospatial-Intelligence Agency. The SRTM data provides baseline information for many types of the worldwide researches. This data is freely available to the public via internet for hydrological modeling and environmental applications.

3.2.2 Soil Data

Soil data of the area was acquired from the harmonized gridded global soil parameter estimation data set that was downloaded from link:

<http://webarchive.iiasa.ac.at/Research/LUC/External-World-soil-database/HTML/>.

The FAO-UNESCO Soil Map of whole World was published in 1978 at 1:5000 000 scale. The harmonization of data and data entry in a GIS was done at the International Institute for Applied System Analysis (IIASA) and the verification of database was done by all partner organizations. The main objective of this product to make its practical use for modelers for perspective studies in agro-ecological zonation, food security, floods, droughts and climate change impacts at about 1 km resolution (30 arc seconds by 30 arc seconds).

The soils were classified on the basis of their textural characteristics. These soils were placed in five textural groups. Each group was identified by the dominant soil names given to the corresponding texture classes and textures as described in Table 3.1.

Table 3.1. Soil types with dominant soil, texture Class and texture in the study area.

Dominant soil	Texture Class	Texture
Cambic Arenosols	Coarse	Sandy Loam, Sand
Haplic Yermosols	Moderately	Sandy Loam, Fine Sandy Loam
Calcaric Regosol	Medium	Sandy Loam, Fine Sandy Loam
Calcic Xerosols	Moderately Fine	Sandy Clay Loam, Clay Loam, Silty
Eutric Cambisol	Fine	Sandy Clay, Silty Clay, Clay.

3.2.3 Land Cover Data

The MODIS Land Cover type data MCD12Q1 is used in this research that provides land cover data by characterizing the worldwide land cover classification system. MCD12Q1 facilitates the users for assessment of land cover type and quality data information.

MCD12Q1 Land Cover product has the classification product which contains the land cover properties obtained from observations of spanning a year's input data of Terra and Aqua-MODIS. This primary land cover product consists of seventeen classes which are defined by the International Geosphere Biosphere Programme (IGBP). This data contains eleven natural vegetation classes, three developed and mosaiced land cover classes and three non-vegetated classes as described in Table 3.2.

Table 3.2. Land cover data with classes, codes and names.

Class	Code	Name
0	WATR	Water
1	FRSE	Evergreen Needleleaf forest
2	FRSD	Evergreen Broadleaf forest
3	FRND	Deciduous Needleleaf forest
4	FRBD	Deciduous Broadleaf forest
5	FRST	Mixed forest
6	CSRB	Closed shrublands
7	OSRB	Open shrublands
8	WVNA	Woody savannas
9	SVNA	Savannas
10	GRL	Grasslands
11	WETL	Permanent wetlands
12	AGRL	Croplands
13	URBN	Urban and built-up
14	AGRR	Cropland/Natural vegetation mosaic
15	SNW	Snow and ice
16	BARR	Barren or sparsely vegetated

3.2.4 In-situ Precipitation Data

Daily rain gauges data in the study area and their locations were obtained from Pakistan Metrological Department (PMD), Islamabad. There are eight PMD stations around the study area, and their names, location and elevation as shown in table 3.3. The daily rainfall data for these stations from 2003 to 2012 was obtained and plotted for individual PMD gauge stations in order to compare with TRMM precipitation for further processing in the SWAT hydrological model.

Table 3.3. PMD Rain gauges with name, location (Latitude/Longitude) and elevation.

No	Name	Latitude	Longitude	Elevation (meter)
1	Bahawalpur	29.4	71.78	119
2	D.G Khan	30.05	70.63	148.1
3	Mianwali	32.58	71.52	210
4	Multan	30.2	71.43	121.95
5	Rahim Yar Khan	28.43	70.32	82.93
6	D.I Khan	31.82	70.92	172.3
7	Barkhan	29.88	69.72	1097
8	Khanpur	28.65	70.68	88.41

3.2.5 Meteorological Data

Daily meteorological data of the middle Indus river basin was used as the input of climate parameters to SWAT model. The meteorological data was requested from Pakistan Metrological Department (PMD), Islamabad. This data included four meteorological parameters Minimum/Maximum Temperature, Wind Speed, Relative Humidity and Solar Radiation from year 2003 to 2012.

3.2.6 In-situ River Discharge Data

Daily discharge data at Chashma and Guddu Barrages was used in the SWAT model as observed discharge sources. Data were obtained from Flood Forecasting Commission (FFC), Islamabad. Daily data cover a time span of 2003 to 2012. FFC discharge data helped to understand and compare the model output discharge over the study area.

3.2.7 Remote Sensing Precipitation Data

Remote Sensing based daily precipitation estimates of TRMM 3B42V7 were downloaded from the following ftp link:

ftp://disc3.nascom.nasa.gov/data/s4pa/TRMM_L3/TRMM_3B42_daily.

The precipitation data is used as a major forcing agent in input SWAT model parameters. The TRMM 3B42V7 rainfall estimates are provided over the latitudes 50° N-S at 0.25° x0.25° grid. The pre-processing of TRMM data is described below:

The daily TRMM 3B42V7 precipitation data from 2003 to 2012 was downloaded in Binary (.BIN) format. Each daily precipitation data Binary file was converted to ASCII format using matlab code given below:

```
fid = fopen('3B42_daily.2009.05.31.7.bin', 'r');
a = fread(fid, 'float','b');
fclose(fid)

data = a';

count = 1;
for i_lat = 1:400
    for j_lon = 1:1440
        lat = -49.875 + 0.25*(i_lat - 1)
        if j_lon <= 720
            lon = 0.125 + 0.25*(j_lon - 1)
        else
            lon = 0.125 + 0.25*(j_lon - 1) - 360.0
        end
        daily_rain_total = data(count)
        count = count + 1;
    end
end
```

Then the ASCII data was converted into Raster format by using ASCII to RASTER conversion tool in ARCGIS for further use.

3.3 COMPARISON OF TRMM AND RAIN GAUGE DATA

In order to use TRMM precipitation data in SWAT model it was compared with in-situ PMD rain gauge data and was validated statistically. The daily and monthly comparison were performed on selected five representative years (2003, 2005, 2008, 2010 and 2012) by observing the daily FFC river stream flow data from 2003 to 2012 at Chashma and Guddu barrages and left all those years which showed similar pattern as shown in Figure 3.2.

The methodology of comparison of TRMM with PMD rain gauge data is described in Figure 3.3. TRMM data (RASTER format) daily cumulative rainfall of whole study area was opened in ARCGIS. Converted PMD eight gauge locations (Bahawalpur, D.G Khan, Mianwali, Multan, D.I Khan, Rahim Yar Khan, Barkhan, Khanpur) to point shape file using add XY data in ARCGIS.

Overlay each day data of TRMM raster and PMD rain gauge points and by using extract value to point tool in ARCGIS to extract values from PMD rain gauge points on TRMM raster data and save as shapefiles. From attribute tables of these shapefiles, all daily TRMM data was arranged in excel to compare it statistically with daily PMD data at all stations in the study area.

3.4 STATISTICAL TEST

Several different types of statistical test indices are in use for comparison of different data sets in hydrology. In this research, the satellite forcing of precipitation was compared with in-situ rain gauge data to logically accept the use of satellite data in the calculation of runoff generation.

Correlation coefficient describes the strength and linear relationship direction between simulated and measured data. The commonly used correlation is Pearson correlation coefficient; it is measured by dividing the covariance by the product of standard deviations of the two variables. It ranges from -1 to 1 , if $CC = 0$, means no linear relationship between two variables. If $CC = 1$ or -1 describe a perfect positive or negative linear relationship.

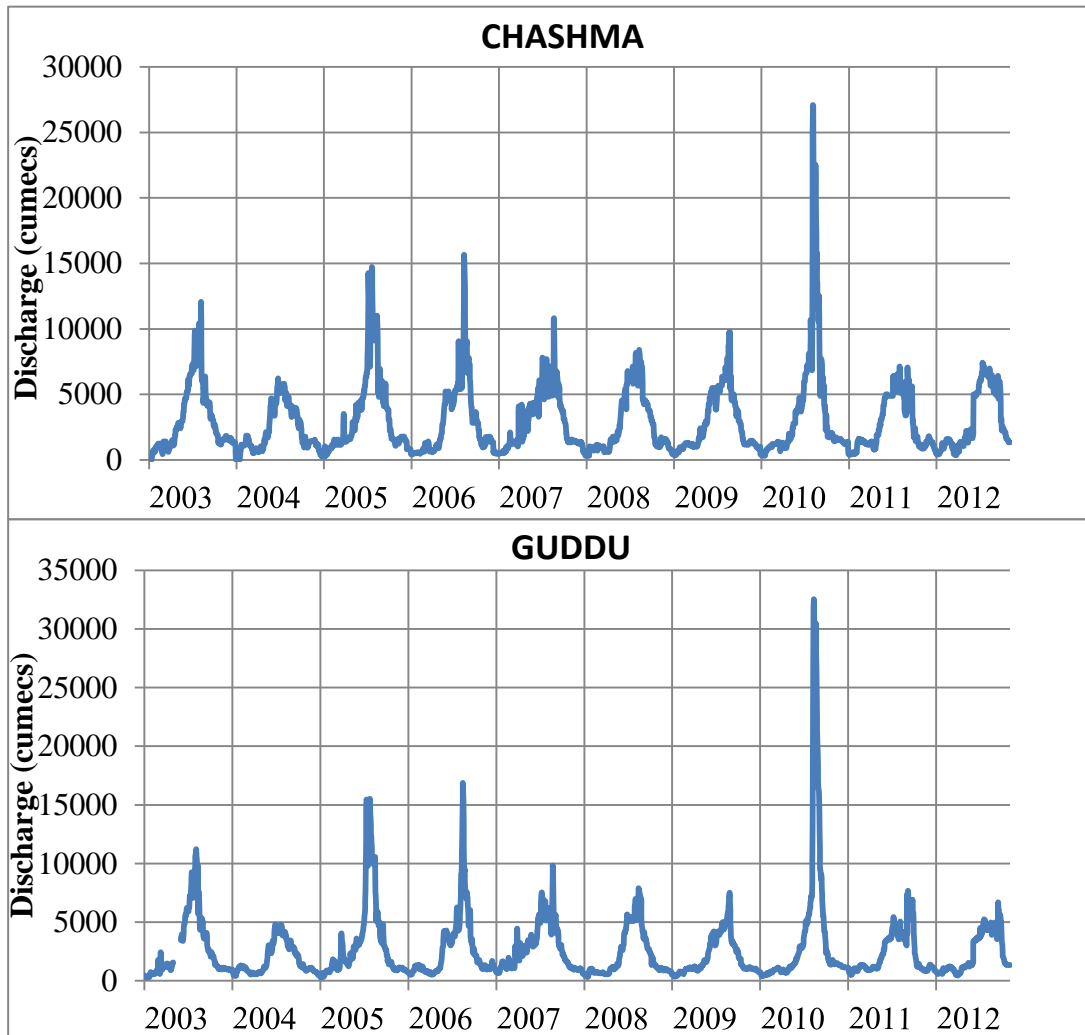


Figure 3.2. Daily stream flow hydrographs from 2003 to 2012 at Chashma and Guddu barrages in cumeecs. The hydrographs of year 2003 and 2007, 2005 and 2006, 2008 and 2009, 2011 and 2012 show similar pattern. (Source: FFC Islamabad, 2014)

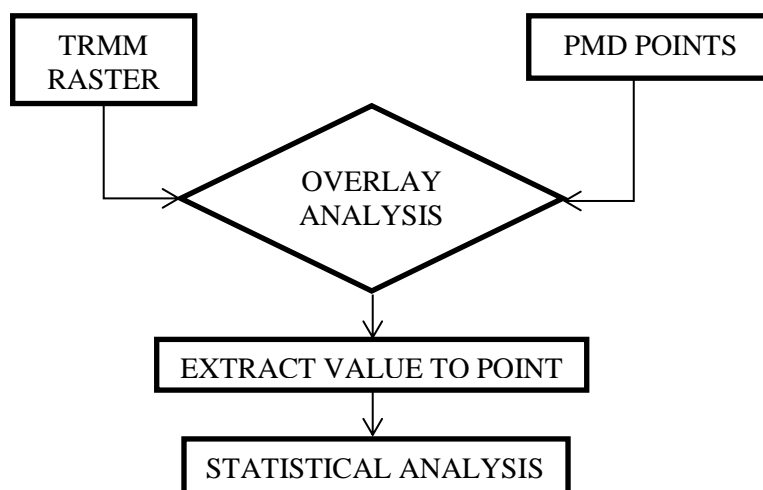


Figure 3.3. Methodology adopted for statistical analysis between TRMM daily precipitation data and in-situ PMD rain gauge data.

If a data with n numbers of ground based observations and n numbers of satellite based values, then the Pearson correlation coefficient can be used to measure the correlation between these two datasets (Santhi et al., 2001).

$$\text{Correlation Coefficient} = \frac{\sum_{i=1}^n (P_G - \bar{P}_G)(P_S - \bar{P}_S)}{\sqrt{\sum_{i=1}^n (P_G - \bar{P}_G)^2} \cdot \sqrt{\sum_{i=1}^n (P_S - \bar{P}_S)^2}}$$

Where

P_G = Ground Based Precipitation

\bar{P}_G = Average Ground Based Precipitation

P_S = Satellite Based Precipitation

\bar{P}_S = Average Satellite Based Precipitation

n = Time Period

The Root Mean Square Error is used to measure the difference between values estimated by a model and actually observed values from the ground. The difference between these two values is called residual and the RMSE combines these differences into a single measure value.

$$\text{Root Mean Square Error} = \sqrt{\frac{1}{n} \sum_{i=1}^n (P_S - P_G)^2}$$

The relative bias is generally known as BIAS which describes the systematic error. The BIAS is used to quantify the systematic error in the satellite data. BIAS indicates whether estimated satellite rainfall is overestimated or underestimated compared to the corresponding observed ground rainfall.

$$\text{Relative Bias \%} = \frac{\sum_{i=1}^n (P_S - P_G)}{\sum_{i=1}^n (P_G)} \times 100$$

3.5 MODEL CALIBRATION

A hydrological model usually needs to calibrate before it is used for an area other than where it was originally developed. The calibration of a model involves modifying values of model input parameters. The values are adjusted within an acceptable range so that the model output results are matched with the observed data. In SWAT hydrological model, the user can manually or automatically calibrate the model. The Manual calibration is based on trial and error method, and by changing one parameter at a time. The adjusting of each parameter and re-running the model to obtain output value that is approximate to the observed value.

A method for manually calibration of SWAT was proposed by Santhi et al. (2001) for river discharge estimation. They proposed that the output results of SWAT model calibration are acceptable if: (i) the simulated flow differs from the observed flow within ± 15 percent; (ii) the coefficient of determination (R^2) is more than 0.60; and (iii) the Nash-Sutcliffe coefficient of efficiency (NSCE) is more than 0.50. The modified form of the suggested procedure as shown in Figure 3.4 was used for calibrating stream flow in this study.

3.6 MODEL PERFORMANCE EVALUATION

There are several evaluation methods in the literature to evaluate the performance of a model. The SWAT model is evaluated using the Nash Sutcliffe Coefficient of Efficiency. NSCE compares the relative magnitude of the residual variance (noise) with the variance (information) of the measured data. The NSCE is commonly used in rainfall runoff modelling to evaluate the model estimated runoff hydrographs (Nash and Sutcliffe, 1970). It enables the efficiency of the model results to be compared with the initial variance of the observed datasets. The

observed and simulated discharge values are compared to estimate the accuracy of the SWAT model.

$$\text{Nash Sutcliffe Coefficient of Efficiency} = 1 - \frac{\sum_{i=1}^n (S_i - O_i)^2}{\sum_{i=1}^n (O_i - \bar{O})^2}$$

Where

O_i = Observed data

\bar{O} = Average Observed data

S_i = Simulated data

The efficiency of NSCE ranges from $-\infty$ to 1, 1 represents an exact match and 0 indicates that the simulated estimations are as accurate as the average of the observed data, whereas less than zero ($-\infty < \text{NSCE} < 0$) represents that the observed average gives better result than the simulated value.

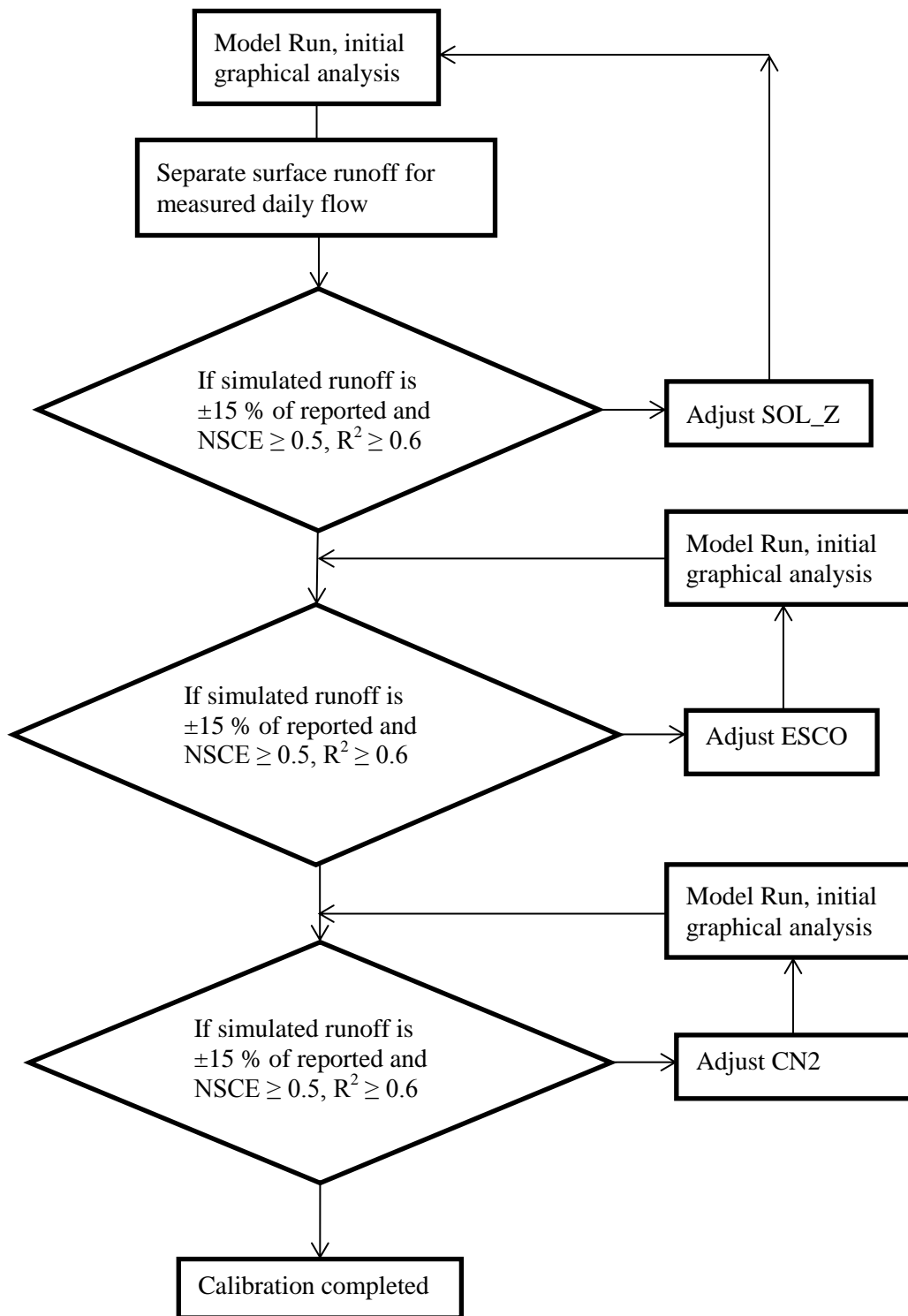


Figure 3.4. Manual calibration procedure for runoff calculation in SWAT model (modified after Santhi et al., 2001).

RESULTS AND DISCUSSION

This chapter discusses the overall results of comparison of satellite based precipitation and gauge data and surface discharge simulated by using SWAT hydrological and FFC discharge data. First section discusses the comparison results of satellite TRMM precipitation and in situ PMD rain gauge data on daily and monthly bases within the study area. In the second section FFC actual stream flow comparison and validation with TRMM remote sensing based surface runoff discharge results from SWAT model were discussed. In the last section, the flood inundation maps using daily model surface runoff on each HRUs in the study area were discussed.

4.1 COMPARISON OF DAILY TRMM PRECIPITATION DATA AND PMD RAIN GAUGE DATA

4.1.1 Scatter Plots and Regression Analysis

The scatter plot is probably the simplest verification tool. Using the 45 degree line or linear line of $y = mx$, where $m = 1$ to represent a better estimate. Scatter diagrams with least squares regression lines were plotted for the TRMM and rain gauge data. If the estimates were perfect, this line would coincide with the 45 degree line (Saw, 2005). A comparison of the slope of the regression line gives a visual representation of the relative quality of the estimates. As the quality decreases, the regression line tends more toward the horizontal (Han, 2010).

Scatter plots and regression lines in Figure 4.1 show the accumulated daily precipitation depths observed by TRMM and PMD at eight rain gauge stations for the year 2003. Figure 4.1(d) shows maximum regression line R^2 value of 0.58 and

4.1(e) shows minimum regression line R^2 value of 0.08. Table 4.1 lists the summary of comparison statistics for year 2003 with average year values of Correlation Coefficient= 0.60, RMSE= 4.37, Relative Bias= -0.23 and R^2 value= 0.38. The results indicate that the relative relationship of TRMM to rain gauge is quite low for the year 2003.

Table 4.1. Statistical results of year 2003 at PMD gauge stations in the area showing Correlation Coefficient, RMSE, Relative Bias and R^2 value (n=365).

2003	Correlation Coefficient	RMSE	Relative Bias	R^2 Value
MIANWALI	0.55	6.14	-0.06	0.30
D.I KHAN	0.70	3.84	-0.27	0.49
D.G KHAN	0.64	3.73	-0.10	0.41
MULTAN	0.76	2.13	-0.17	0.58
BARKHAN	0.28	4.40	-0.46	0.08
BAHAWALPUR	0.59	5.30	-0.52	0.35
KHANPUR	0.67	5.29	-0.08	0.45
RAHIM YAR KHAN	0.58	4.13	-0.16	0.34
AVERAGE	0.60	4.37	-0.23	0.38

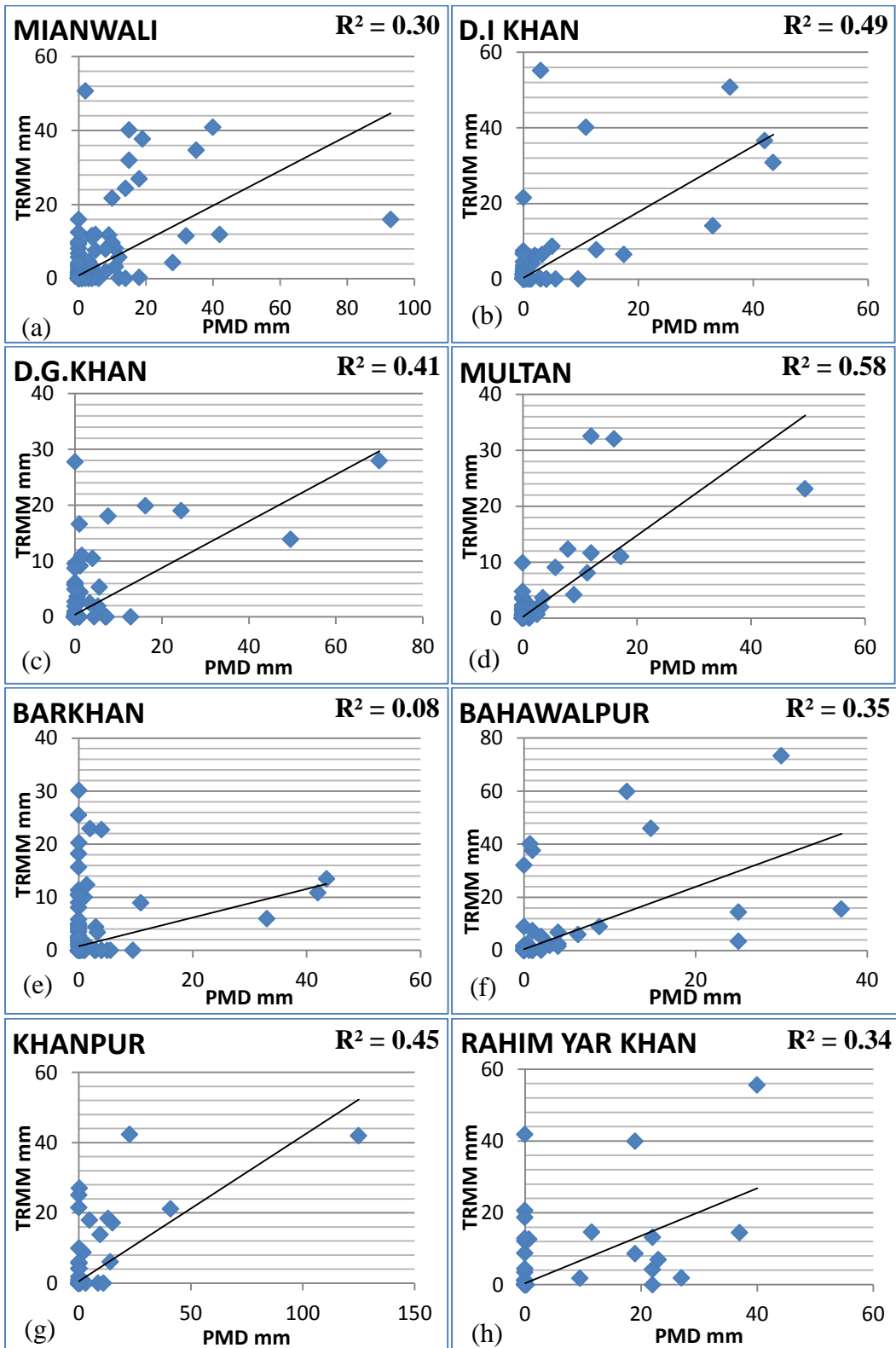


Figure 4.1. Scatter plots with regression line of daily TRMM versus PMD rain gauge data of 2003 showing maximum R^2 value 0.58 at Multan and minimum value 0.08 at Barkhan (n=365).

Scatter plots and regression lines in Figure 4.2 show the accumulated daily precipitation depths observed by TRMM and PMD at eight rain gauge stations for the year 2005. Figure 4.2(f) shows maximum regression line R^2 value of 0.68 and 4.2(c) shows minimum regression line R^2 value of 0.22. Table 4.2 lists the summary of comparison statistics for year 2005 with average year values of Correlation Coefficient= 0.69, RMSE= 3.58, Relative Bias= -0.20 and R^2 value= 0.48. The results of year 2005 indicate that the relative relationship of TRMM to rain gauge is better than year 2003.

Table 4.2. Statistical results of year 2005 at PMD gauge stations in the area showing Correlation Coefficient, RMSE, Relative Bias and R^2 value (n=365).

2005	Correlation Coefficient	RMSE	Relative Bias	R^2 Value
MIANWALI	0.65	6.41	-0.11	0.42
D.I KHAN	0.73	4.57	0.27	0.53
D.G KHAN	0.47	4.08	-0.34	0.22
MULTAN	0.71	3.58	-0.04	0.51
BARKHAN	0.69	5.00	-0.12	0.47
BAHAWALPUR	0.82	1.84	-0.19	0.68
KHANPUR	0.67	1.60	-0.45	0.45
RAHIM YAR KHAN	0.74	1.54	-0.58	0.54
AVERAGE	0.69	3.58	-0.20	0.48

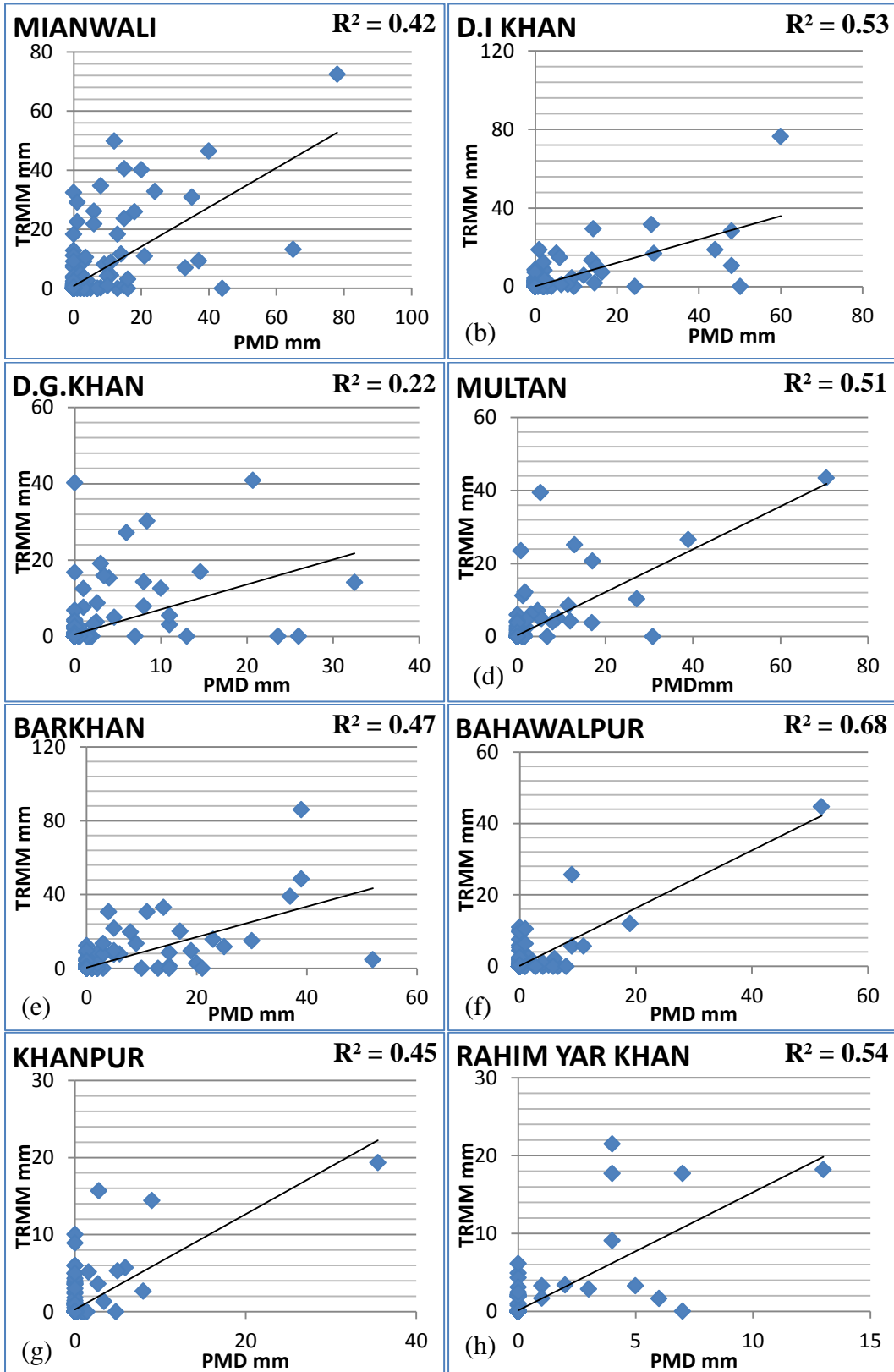


Figure 4.2. Scatter plots with regression line of daily TRMM versus PMD rain gauge data of 2005 showing maximum R^2 value 0.68 at Bahawalpur and minimum value 0.22 at D.G Khan (n=365).

Scatter plots and regression lines in Figure 4.3 show the accumulated daily precipitation depths observed by TRMM and PMD at eight rain gauge stations for the year 2008. Figure 4.3(g) shows maximum regression line R^2 value of 0.69 and 4.3(e) shows minimum regression line R^2 value of 0.13. Table 4.3 lists the summary of comparison statistics for year 2008 with average year values of Correlation Coefficient= 0.66, RMSE= 4.77, Relative Bias= -0.04 and R^2 value= 0.45. The results of year 2008 indicate that the relative relationship of TRMM to rain gauge is better than year 2003 but lower than year 2005.

Table 4.3. Statistical results of year 2008 at PMD gauge stations in the area showing Correlation Coefficient, RMSE, Relative Bias and R^2 value (n=366).

2008	Correlation Coefficient	RMSE	Relative Bias	R^2 Value
MIANWALI	0.56	7.73	-0.08	0.31
D.I KHAN	0.61	5.48	0.15	0.37
D.G KHAN	0.63	5.60	0.12	0.40
MULTAN	0.67	3.12	-0.16	0.45
BARKHAN	0.36	5.30	-0.64	0.13
BAHAWALPUR	0.79	3.74	0.23	0.62
KHANPUR	0.83	3.98	0.12	0.69
RAHIM YAR KHAN	0.80	3.20	-0.03	0.64
AVERAGE	0.66	4.77	-0.04	0.45

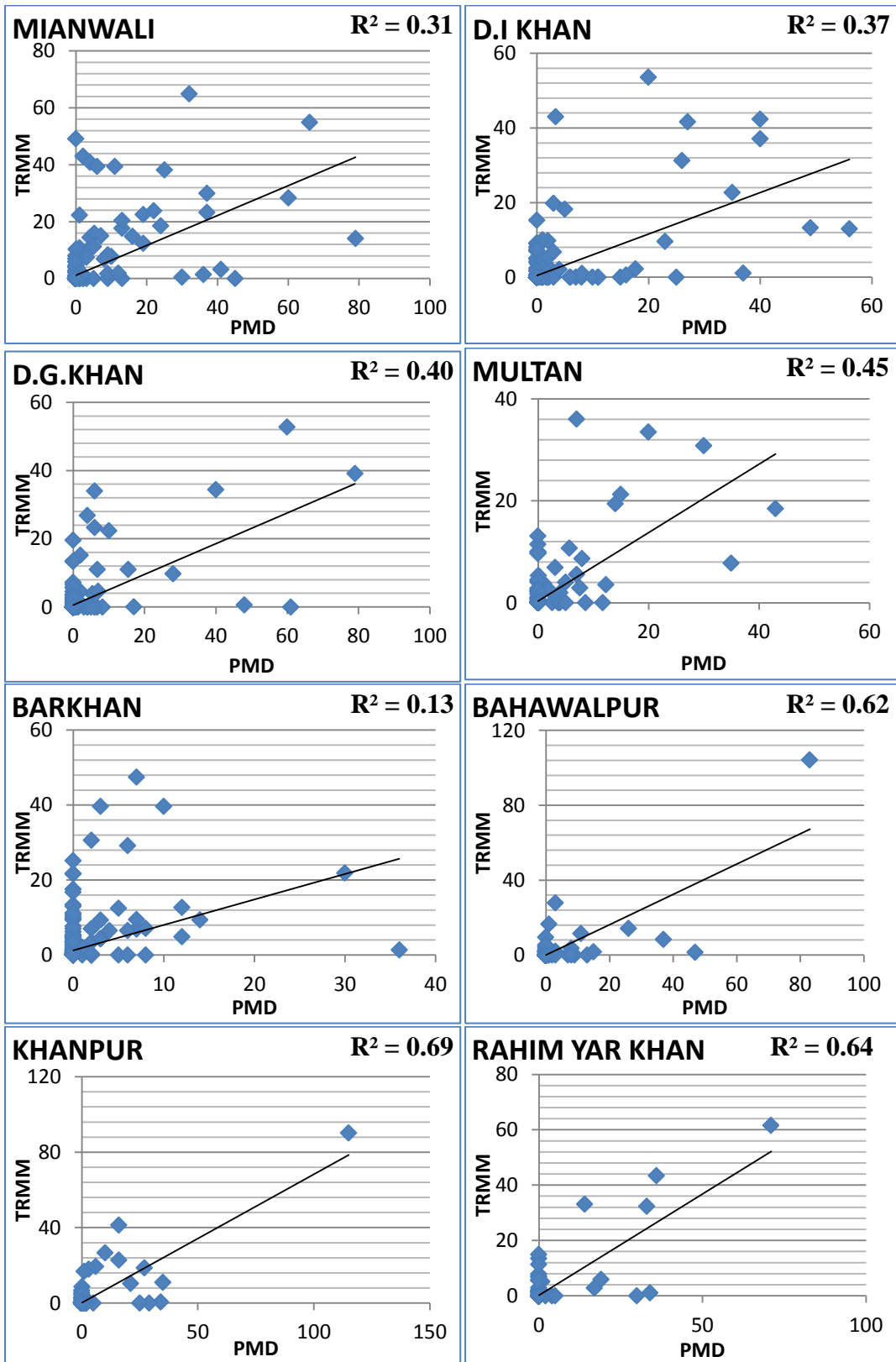


Figure 4.3. Scatter plots with regression line of daily TRMM versus PMD rain gauge data of 2008 showing maximum R^2 value 0.69 at Khanpur and minimum value 0.13 at Barkhan (n=366).

Scatter plots and regression lines in Figure 4.4 show the accumulated daily precipitation depths observed by TRMM and PMD at eight rain gauge stations for the year 2010. Figure 4.4(c) shows maximum regression line R^2 value of 0.65 and 4.4(a) shows minimum regression line R^2 value of 0.17. Table 4.4 lists the summary of comparison statistics for year 2010 with average year values of Correlation Coefficient= 0.61, RMSE= 5.37, Relative Bias= -0.13 and R^2 value= 0.38. The results of year 2010 indicate that the relative relationship of TRMM to rain gauge is low like in year 2003.

Table 4.4. Statistical results of year 2010 at PMD gauge stations in the area showing Correlation Coefficient, RMSE, Relative Bias and R^2 value (n=365).

2010	Correlation Coefficient	RMSE	Relative Bias	R^2 Value
MIANWALI	0.41	14.28	0.30	0.17
D.I KHAN	0.77	0.15	0.07	0.59
D.G KHAN	0.81	3.16	-0.14	0.65
MULTAN	0.57	6.06	-0.32	0.32
BARKHAN	0.54	5.26	-0.13	0.30
BAHAWALPUR	0.53	4.13	-0.44	0.28
KHANPUR	0.57	6.19	-0.01	0.32
RAHIM YAR KHAN	0.67	3.69	-0.38	0.44
AVERAGE	0.61	5.37	-0.13	0.38

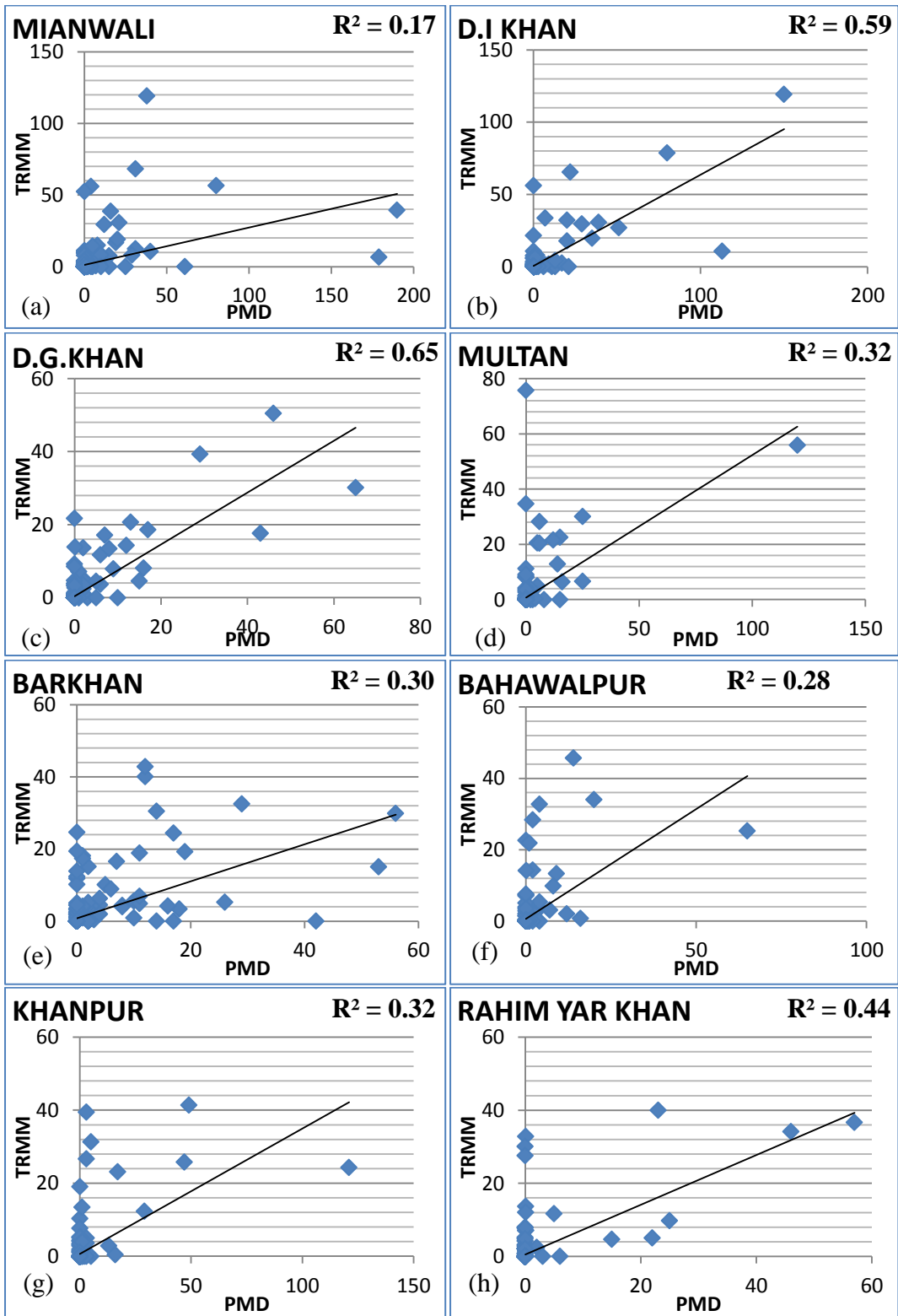


Figure 4.4. Scatter plots with regression line of daily TRMM versus PMD rain gauge data of 2010 showing maximum R^2 value 0.65 at D.G Khan and minimum value 0.22 at Mianwali (n=365).

Scatter plots and regression lines in Figure 4.5 show the accumulated daily precipitation depths observed by TRMM and PMD at eight rain gauge stations for the year 2012. Figure 4.5(f) shows maximum regression line R^2 value of 0.74 and 4.5(a) shows minimum regression line R^2 value of 0.24. Table 4.5 lists the summary of comparison statistics for year 2012 with average year values of Correlation Coefficient= 0.64, RMSE= 5.38, Relative Bias= -0.09 and R^2 value= 0.43. The results of year 2012 indicate that the relative relationship of TRMM to rain gauge is good than all previous years 2003, 2005, 2008 and 2010.

Table 4.5. Statistical results of year 2012 at PMD gauge stations in the area showing Correlation Coefficient, RMSE, Relative Bias and R^2 value (n=366).

2012	Correlation Coefficient	RMSE	Relative Bias	R^2 Value
MIANWALI	0.49	7.11	-0.18	0.24
D.I KHAN	0.77	4.66	-0.15	0.60
D.G KHAN	0.53	4.73	-0.31	0.28
MULTAN	0.80	3.30	-0.06	0.64
BARKHAN	0.58	4.20	-0.05	0.33
BAHAWALPUR	0.86	3.15	-0.14	0.74
KHANPUR	0.55	9.07	0.27	0.31
RAHIM YAR KHAN	0.55	6.80	-0.11	0.31
AVERAGE	0.64	5.38	-0.09	0.43

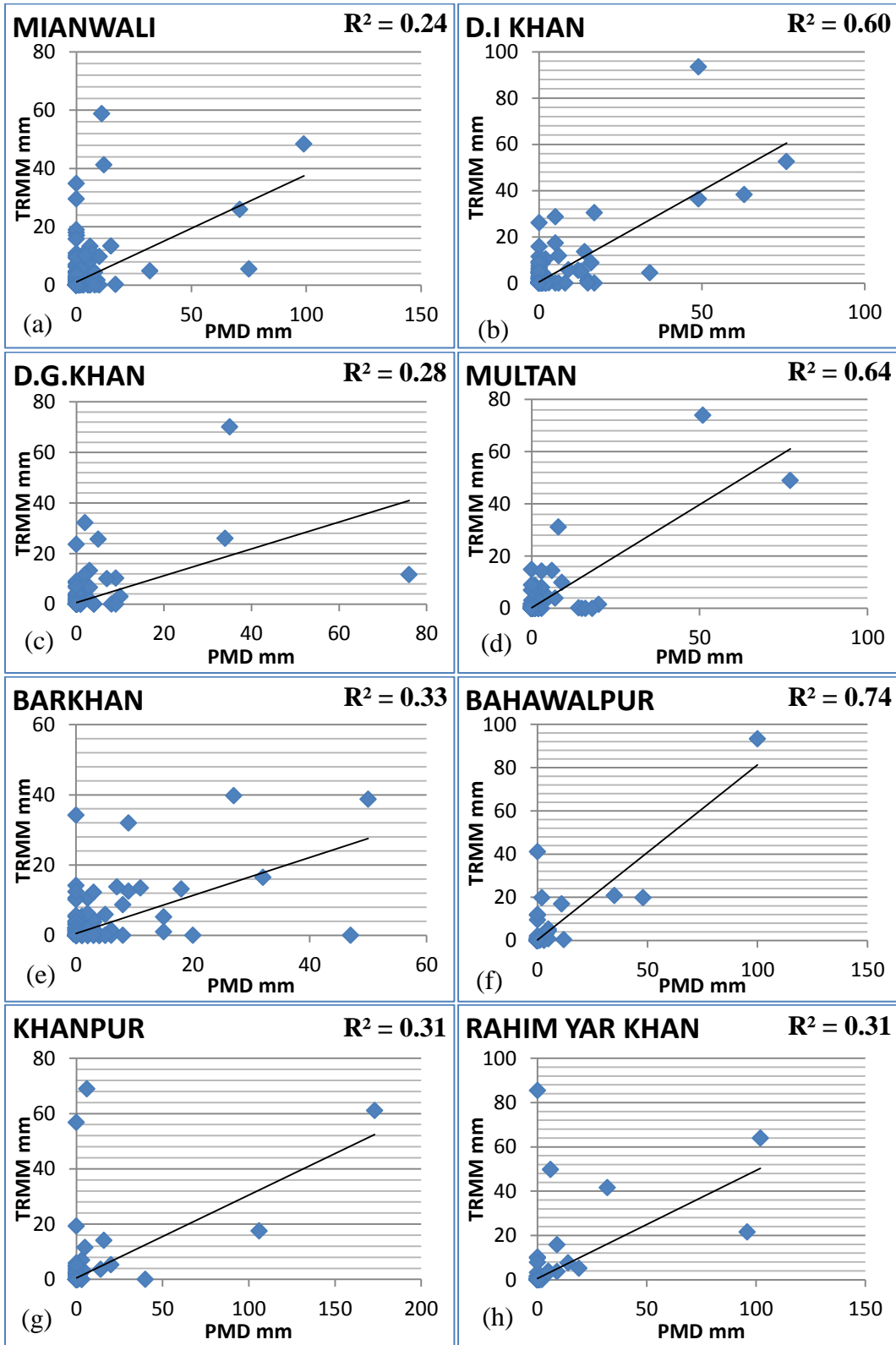


Figure 4.5. Scatter plots with regression line of daily TRMM versus PMD rain gauge data of 2012 showing maximum R^2 value 0.74 at Bahawalpur and minimum value 0.24 at Mianwali (n=366).

Table 4.6. Five years daily average statistical results at all PMD gauge stations showing Correlation Coefficient, RMSE, Relative Bias and R² value.

Years	Correlation Coefficient	RMSE	Relative Bias	R² Value
2003	0.60	4.37	-0.23	0.38
2005	0.69	3.58	-0.20	0.48
2008	0.66	4.77	-0.04	0.45
2010	0.61	5.37	-0.13	0.38
2012	0.64	5.38	-0.09	0.43
AVERAGE	0.64	4.69	-0.14	0.42

Table 4.6 lists the overall summary comparison statistics at eight gauges for all five years 2003, 2005, 2008, 2010 and 2012 with average values of Correlation Coefficient= 0.64, RMSE= 4.69, Relative Bias= -0.14 and R²= 0.42. These average year values represent whole study area response over the selected duration 2003 to 2012. These results indicate that the relative relationship of daily TRMM precipitation to rain gauge is not very good (R²=0.42) because the average value of coefficient of determination (R²) should be more than 0.60 (Santhi et al., 2001).

The comparison of TRMM 3B42V7 with PMD rain gauge data is low due to probably following main reasons:

1. The satellite TRMM failure of estimation of local development of clouds and rain common during monsoon season.
2. The difference in time of measurement of rainfall between satellite (after every 3 hours) and PMD gauges (daily at~8 AM) produces the major difference in these two data sets i.e the rain from 12 AM to 8 AM should be counted in the previous day.

4.2 COMPARISON OF MONTHLY TRMM PRECIPITATION DATA AND PMD RAIN GAUGE DATA

As a general rule R^2 of 0.50 values and above are considered here as good correlation. But the daily comparison results over the middle Indus river basin for years 2003, 2005, 2008, 2010 and 2012 shows average R^2 value 0.38, 0.48, 0.45, 0.38 and 0.43 respectively. This low value of R^2 for daily data is due to uneven distribution of rainfall in the study area. There is a large variation of rainfall in Mianwali, Barkhan, D.G Khan, D.I Khan, Multan, Bahawalpur, Khanpur and Rahim Yar Khan throughout the year. The intensity of rainfall decreases from north to south. Mianwali receives maximum rainfall of average about more than 600 mm per year and Rahim Yar Khan receives the minimum rainfall of about 250 mm per year in the study area. On the other hand the correlation between monthly precipitation estimates of TRMM and in-situ rain gauge data shows better results than the daily precipitation estimates. This indicates that the TRMM 3B42V7 monthly cumulative estimates are better suited for use in hydrological modeling. They compensate for the finer time scale variation error in daily precipitation.

The bar graphs in Figure 4.6 show the accumulated monthly precipitation depths observed by TRMM and PMD at eight rain gauge locations for the year 2003. Table 4.7 lists the summary of monthly comparison statistics for year 2003. It shows maximum regression line R^2 value= 0.97 at D.I Khan and minimum regression line $R^2 = 0.52$ at D.G Khan with average year (2003) value of Correlation Coefficient= 0.89, RMSE= 3.90, Relative Bias= 0.37 and $R^2= 0.77$. These average values are representing the whole study area results for the year 2003. The regression line graphs with R^2 values ranges from 0.52 - 0.97 of year

2003 are placed in Appendix 1. The results are indicating that the relative relationship of monthly TRMM to rain gauge for the year 2003 is very good.

Table 4.7. Monthly statistical results of year 2003 at PMD gauge stations in the area showing Correlation Coefficient, RMSE, Relative Bias and R² value (n=365).

2003	Correlation Coefficient	RMSE	Relative Bias	R² Value
MIANWALI	0.79	5.49	0.12	0.62
D.I KHAN	0.98	1.99	0.36	0.97
D.G KHAN	0.72	4.53	1.15	0.52
MULTAN	0.89	2.05	0.21	0.78
BARKHAN	0.91	2.57	-0.03	0.84
BAHAWALPUR	0.94	9.30	1.10	0.64
KHANPUR	0.96	2.21	0.09	0.93
RAHIM YAR KHAN	0.94	3.10	-0.04	0.88
AVERAGE	0.89	3.90	0.37	0.77

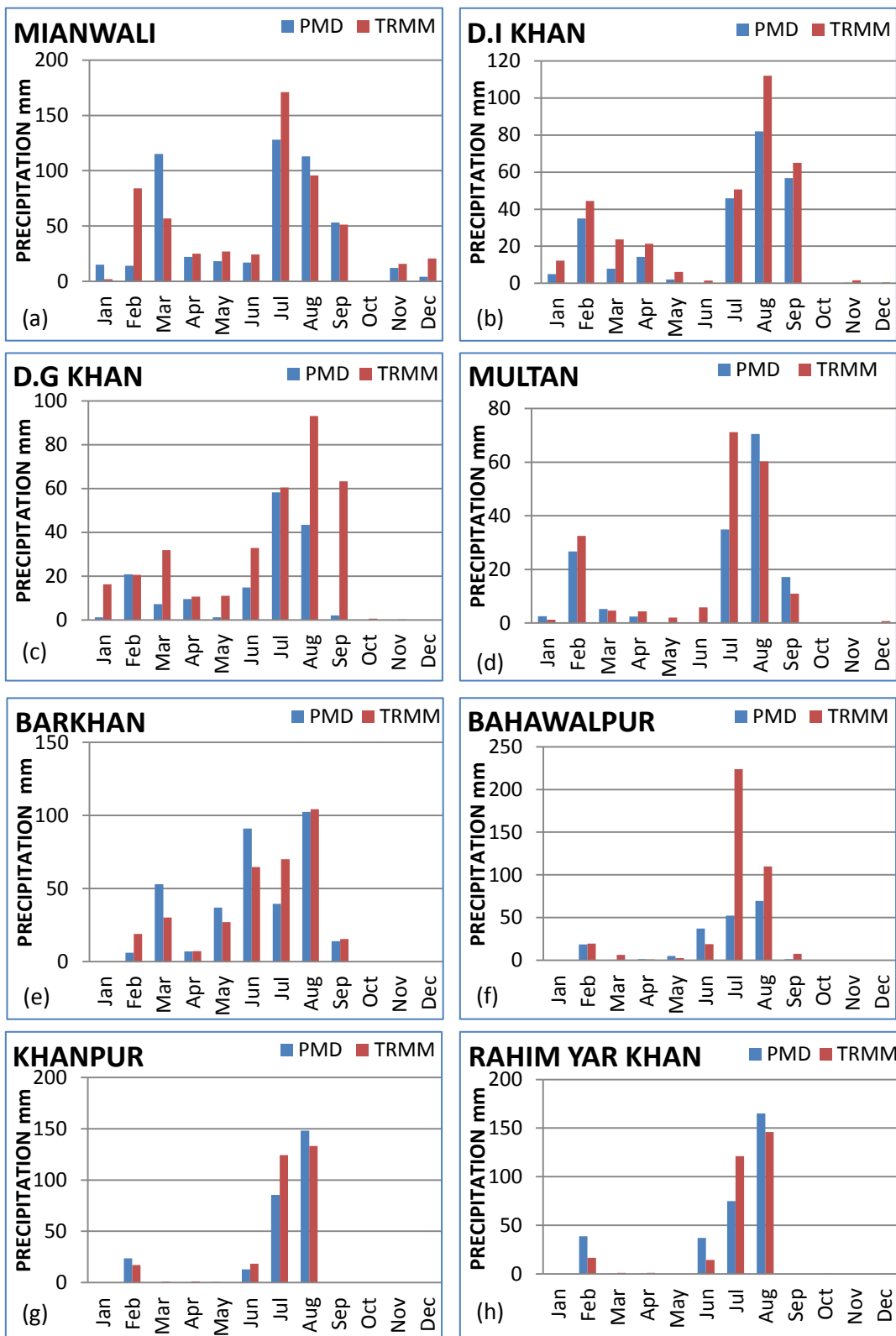


Figure 4.6. Bar graphs of monthly TRMM versus rain gauge show the bimodal behavior in the area for year 2003.

The bar graphs in Figure 4.7 show the accumulated monthly precipitation depths observed by TRMM and PMD at eight rain gauge locations for the year 2005. Table 4.8 lists the summary of monthly comparison statistics for year 2005. It shows the maximum R^2 value= 0.92 at Mianwali and minimum R^2 = 0.68 at Rahim Yar Khan with average year (2005) value of Correlation Coefficient= 0.89, RMSE= 2.89, Relative Bias= 0.38 and R^2 = 0.80. These average values are representing the whole study area results for the year 2005. The regression line graphs with R^2 values ranges from 0.68 - 0.92 of year 2005 are placed in Appendix 2. These results are indicating that the relative relationship of monthly TRMM to rain gauge is very good and are better than year 2003.

Table 4.8. Monthly statistical results of year 2005 at PMD gauge stations in the area showing Correlation Coefficient, RMSE, Relative Bias and R^2 value (n=365).

2005	Correlation Coefficient	RMSE	Relative Bias	R^2 Value
MIANWALI	0.96	3.44	0.12	0.92
D.I KHAN	0.88	4.27	-0.21	0.78
D.G KHAN	0.90	3.43	0.51	0.80
MULTAN	0.90	2.59	0.04	0.81
BARKHAN	0.94	3.5	0.14	0.88
BAHAWALPUR	0.87	2.06	0.23	0.76
KHANPUR	0.86	1.87	0.82	0.73
RAHIM YAR KHAN	0.83	2.01	1.37	0.68
AVERAGE	0.89	2.89	0.38	0.80

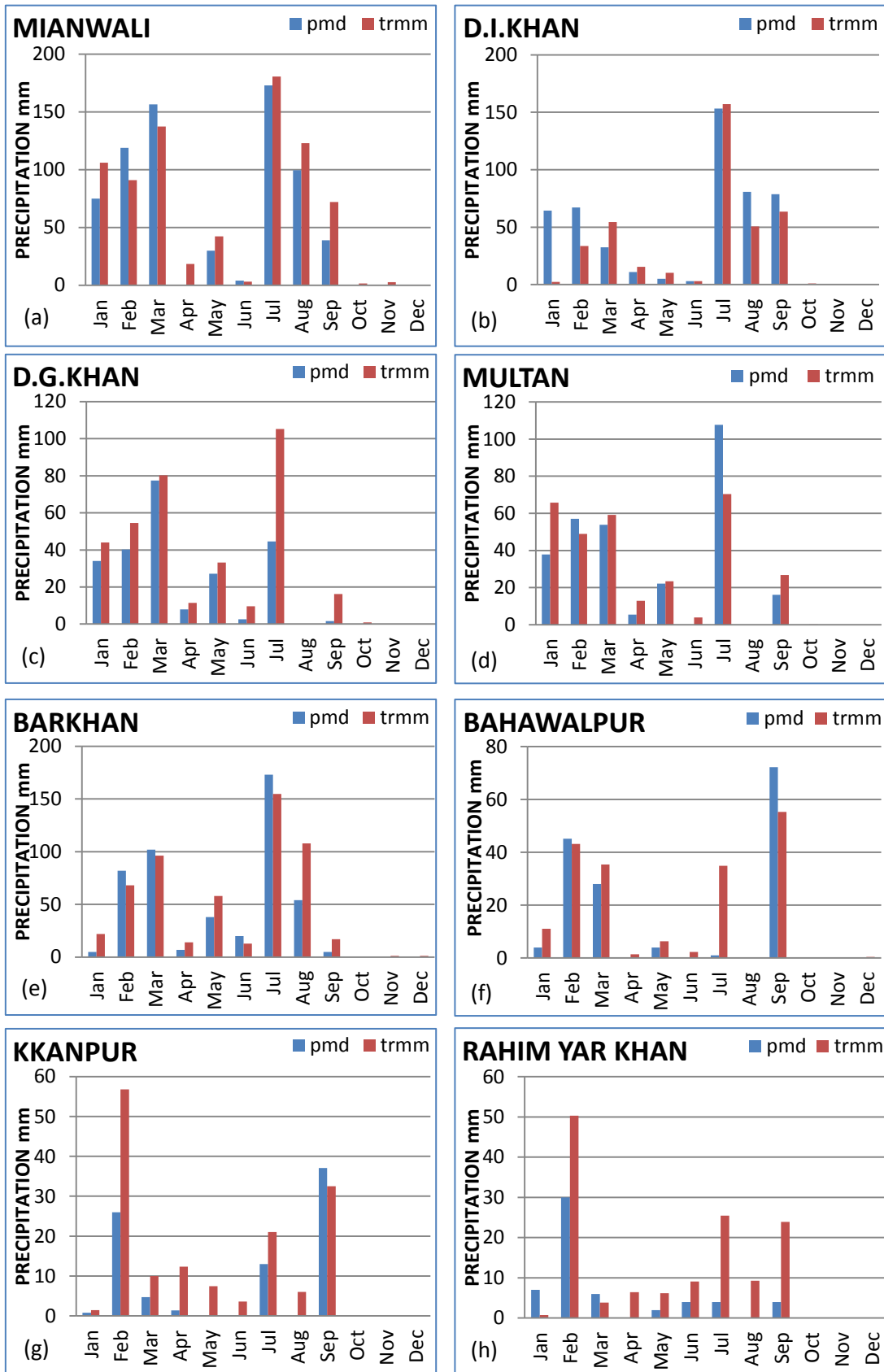


Figure 4.7. Bar graphs of monthly TRMM versus rain gauge show the bimodal behavior in the area for year 2005.

The bar graphs in Figure 4.8 show the accumulated monthly precipitation depths observed by TRMM and PMD at eight rain gauge locations for the year 2008. Table 4.9 lists the summary of monthly comparison statistics for year 2008 which shows the maximum R^2 value= 0.96 at Khanpur and minimum R^2 = 0.68 at Multan with average year (2008) value of Correlation Coefficient= 0.91, RMSE= 3.68, Relative Bias= 0.01 and R^2 value= 0.84. The regression line graphs with R^2 values ranges from 0.68 - 0.96 of year 2008 are placed in Appendix 3. These results are indicating that the relative relationship of year 2008 monthly TRMM to rain gauge is better than year 2005.

Table 4.9. Monthly statistical results of year 2008 at PMD gauge stations in the area showing Correlation Coefficient, RMSE, Relative Bias and R^2 value (n=366).

2008	Correlation Coefficient	RMSE	Relative Bias	R^2 Value
MIANWALI	0.87	6.62	0.09	0.75
D.I KHAN	0.97	2.74	-0.13	0.95
D.G KHAN	0.84	4.50	-0.11	0.71
MULTAN	0.82	3.06	0.20	0.68
BARKHAN	0.96	3.53	0.15	0.93
BAHAWALPUR	0.91	3.32	-0.19	0.84
KHANPUR	0.98	3.75	0.01	0.96
RAHIM YAR KHAN	0.94	1.96	0.03	0.88
AVERAGE	0.91	3.68	0.01	0.84

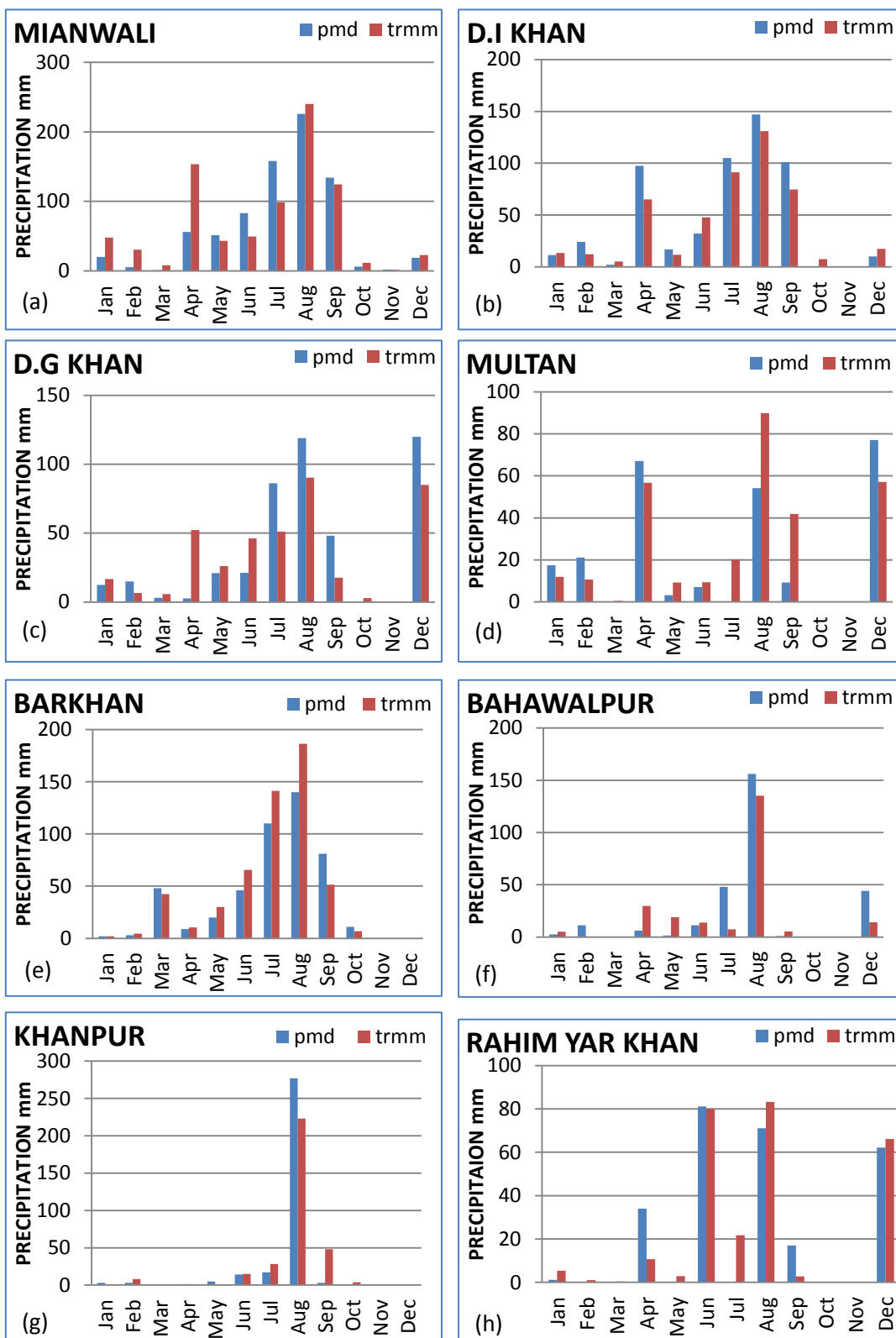


Figure 4.8. Bar graphs of monthly TRMM versus rain gauge show the bimodal behavior in the area for year 2008.

The bar graphs in Figure 4.9 show the accumulated monthly precipitation depths observed by TRMM and PMD at eight rain gauge locations for the year 2010. Table 4.10 lists the summary of monthly comparison statistics for year 2010 which shows maximum R^2 value= 0.96 at Multan and minimum R^2 value= 0.70 at Barkhan with average year (2010) value of Correlation Coefficient= 0.92, RMSE= 6.35, Relative Bias= 0.42 and R^2 value= 0.85. The regression line graphs with R^2 values ranges from 0.70- 0.96 of year 2010 are placed in Appendix 4. These results are indicating that the relative relationship of monthly TRMM to rain gauge is very good for the year 2010 and is better than 2003, 2005 and 2008.

Table 4.10. Monthly statistical results of year 2010 at PMD gauge stations in the area showing Correlation Coefficient, RMSE, Relative Bias and R^2 value (n=365).

2010	Correlation Coefficient	RMSE	Relative Bias	R^2 Value
MIANWALI	0.85	15.11	-0.23	0.72
D.I KHAN	0.93	7.81	-0.07	0.86
D.G KHAN	0.97	2.60	0.16	0.93
MULTAN	0.98	4.62	0.47	0.96
BARKHAN	0.83	10.40	1.77	0.70
BAHAWALPUR	0.96	3.61	0.79	0.92
KHANPUR	0.91	2.87	-0.11	0.83
RAHIM YAR KHAN	0.97	3.80	0.60	0.94
AVERAGE	0.92	6.35	0.42	0.85

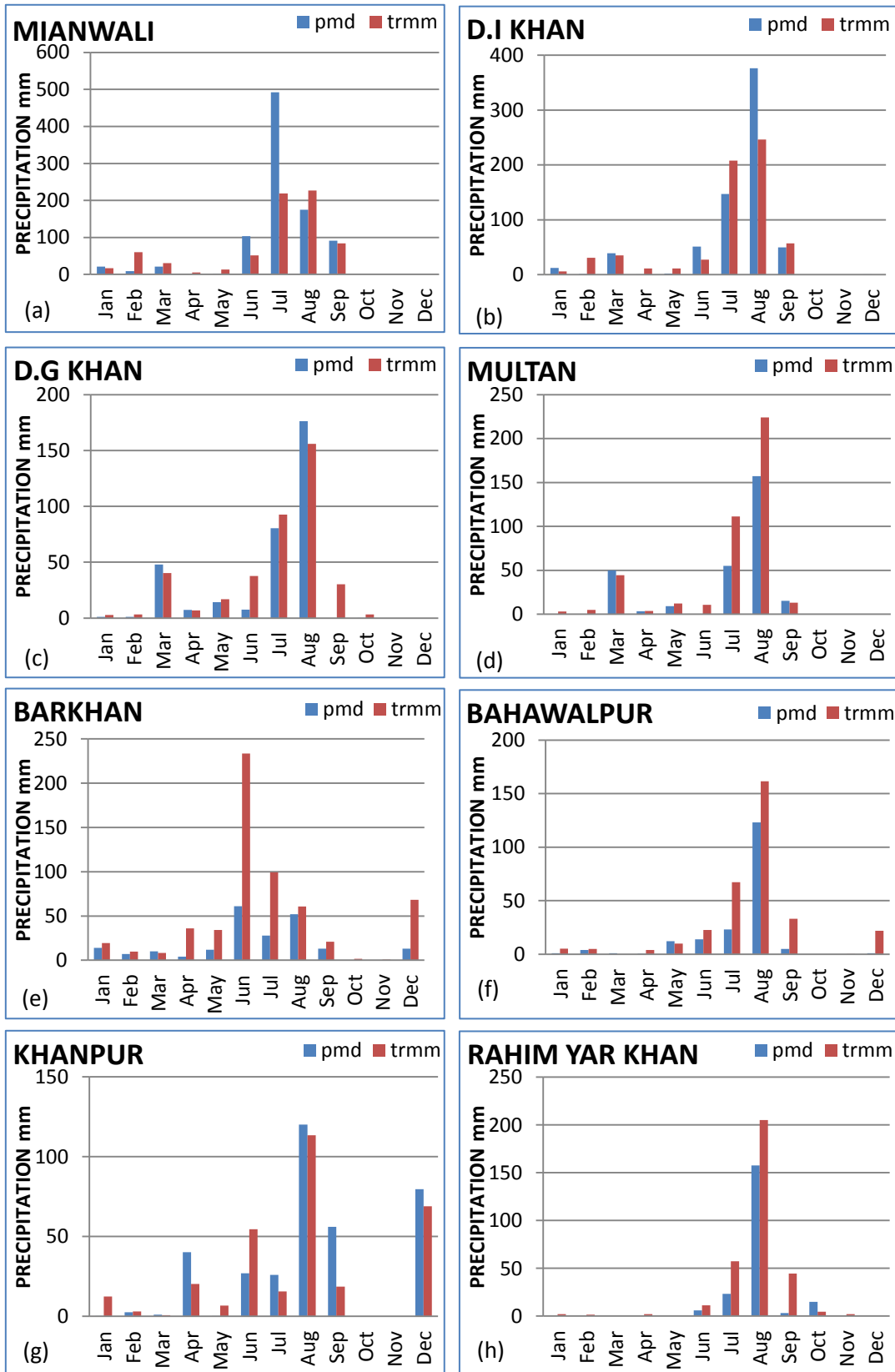


Figure 4.9. Bar graphs of monthly TRMM versus rain gauge show the bimodal behavior in the area for year 2010.

The bar graphs in Figure 4.10 show the accumulated monthly precipitation depths observed by TRMM and PMD at eight rain gauge locations for the year 2012. Table 4.11 lists the summary of monthly comparison statistics for year 2012 which shows the maximum R^2 value= 0.99 at Khanpur and Rahim Yar Khan and minimum R^2 value= 0.63 at Barkhan with average year (2012) value of Correlation Coefficient= 0.92, RMSE= 3.53, Relative Bias= 0.13 and R^2 value= 0.86. The regression line graphs with R^2 values ranges from 0.63 - 0.99 of year 2012 are placed in Appendix 5. These results are indicating that the relative relationship of monthly TRMM to rain gauge is better than all the previous years (2003, 2005, 2008 and 2010).

Table 4.11. Monthly statistical results of year 2012 at PMD gauge stations in the area showing Correlation Coefficient, RMSE, Relative Bias and R^2 value (n=366).

2012	Correlation Coefficient	RMSE	Relative Bias	R^2 Value
MIANWALI	0.85	5.09	0.22	0.73
D.I KHAN	0.94	3.27	0.18	0.88
D.G KHAN	0.94	2.93	0.46	0.89
MULTAN	0.95	2.53	0.06	0.89
BARKHAN	0.79	5.20	0.05	0.63
BAHAWALPUR	0.93	3.16	0.16	0.87
KHANPUR	0.99	4.00	-0.21	0.99
RAHIM YAR KHAN	0.99	2.06	0.13	0.99
AVERAGE	0.92	3.53	0.13	0.86

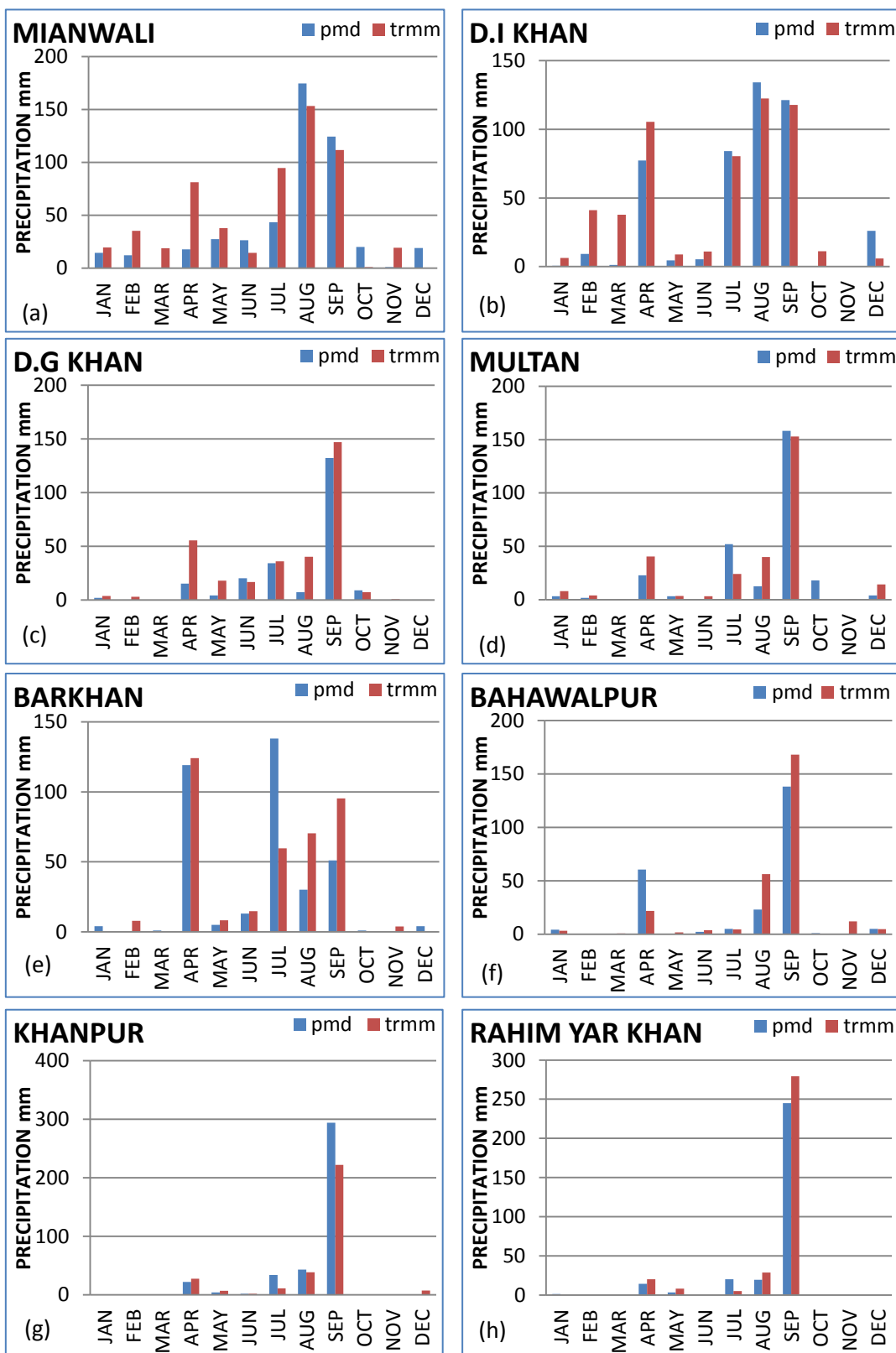


Figure 4.10. Bar graphs of monthly TRMM versus rain gauge show the bimodal behavior in the area for year 2012.

Table 4.12. Five years monthly average statistical results at PMD gauge stations in the area showing Correlation Coefficient, RMSE, Relative Bias and R² value.

Years	Correlation Coefficient	RMSE	Relative Bias	R² Value
2003	0.89	3.90	0.37	0.77
2005	0.89	2.89	0.38	0.80
2008	0.91	3.68	0.01	0.84
2010	0.92	6.35	0.42	0.85
2012	0.92	3.53	0.13	0.86
AVERAGE	0.91	4.07	0.26	0.82

Table 4.12 lists the overall summary of monthly comparison statistics at eight gauges for five years 2003, 2005, 2008, 2010 and 2012 with average value of Correlation Coefficient= 0.91, RMSE= 4.07, Relative Bias= 0.26 and R²= 0.82. These average values are representing whole study area response over the selected duration 2003 to 2012. These results are clearly indicating that the relative relationship of monthly TRMM precipitation to rain gauge is very good.

The monthly graphs for five years show that the satellite is overestimating the total rainfall. This leads to underestimates of higher rainfall. Chokngamwong and Chiu (2006) and Islam and Uyeda (2008) experienced similar trends in Thailand and Bangladesh, respectively. Chokngamwong and Chiu (2006) found that the satellite overestimated at the low and mid rainfall rate range (<400 mm month⁻¹), but underestimated at the higher end (>400 mm month⁻¹). So the satellite TRMM 3B42 V7 data can be used for hydrological modeling and other research purposes instead of PMD rain gauges data.

4.3 MODEL CALIBRATION AND VALIDATION

The SWAT hydrological model was set up for the Middle Indus river basin by following the procedure described in the SWAT user guide. ArcSWAT version 2012.10_14 model built for ArcMap 10.1 was used for this study. A manual calibration was done on most sensitive parameters that affect the runoff simulated by model. Following four parameters (Table 4.7) were identified which greatly effects the runoff values of simulation.

This study was conducted on Middle Indus river basin from Chashma to Guddu barrage. First of all watershed and sub-watersheds parameters were calculated which was further divided into 31 HRUs based on soil and land cover data using threshold of five per cent for both soil and land cover during HRUs characterization. SWAT Model was calibrated to generate discharge using water balance equation.

Table 4.13. Default and adjusted ranges of SWAT model parameters used in calibration (Luzio et al., 2002).

Parameter	Description	Parameter Range	Adjusted Parameter
ESCO	Soil evaporation compensation factor	0-1	0.50
CN2	SCS runoff curve number	35-98	70
SOL_K	Saturated hydraulic conductivity (mm/hr)	Depends on soil texture	12-101
SOL_AWC	Available water capacity of soil layer (mm/mm)	Depends on soil texture	0.13-0.15

Both temporal and spatial calibration and validation of model was done. The SWAT model was calibrated from year 2003 to 2010 on Middle Indus river basin. The calibration process was done by adjusting the sensitive input parameters of model, to achieve the best results between the model simulated and FFC observed discharge data. Since the outlet stream discharge values are regulated by water management authorities and stream flow in-situ numbers do not represent natural stream runoff. Therefore an exercise was attempted to estimate the portion of stream flow impacting the stream runoff at the outlet point by trial and error method. The water management authorities at Chashma, Kalabagh and Guddu regulate the outflow based on requirement from irrigation departments to supply water in the canals. At Guddu the stream flow includes a component each from the precipitation between Chashma and Guddu topographic sub-watershed and from Chashma outlet. Since there is no obvious point from where Chashma out value could be entered in the SWAT model, the value is manually added to the simulated discharge value of SWAT model at Guddu outlet point.

Model daily discharge results were compared with daily stream flow data of Guddu barrage located on the most downstream point of the study area. Model was run for period of ten years from 2003 to 2012. First eight years from 2003 to 2010 were used as a model warm up period for calibration and 2011 and 2012 were used for validation of the model. Table 4.14 shows the model calibration and validation results with R^2 value=0.72 and 0.73, NSCE= 0.69 and 0.65 and Relative BIAS= -0.06 and 0.18 respectively. The calibration and validation line graphs and Table 4.14 show that hydrological model was representing significantly good volumetric discharge results. In calibration there is slightly underestimating of the

peak discharge values in monsoon season but are well estimated in validation period. The rapid decrease in observed FFC discharge after monsoon season did not match with model discharge because water is stored for summers and managed in barrages or dams for irrigation purposes for future use.

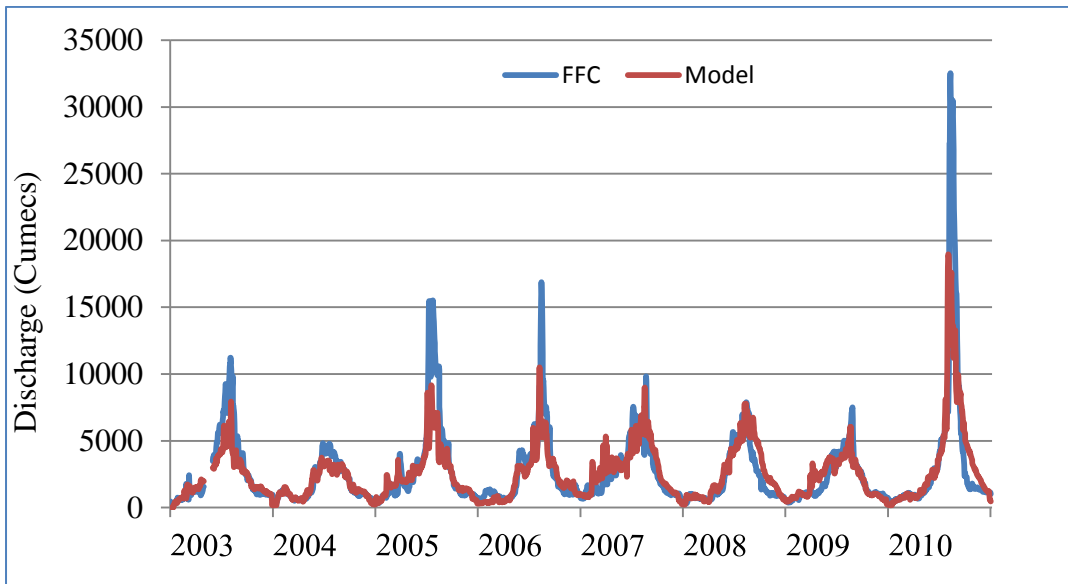


Figure 4.11. Calibration results of SWAT model on Middle Indus River basin from 2003 to 2010.

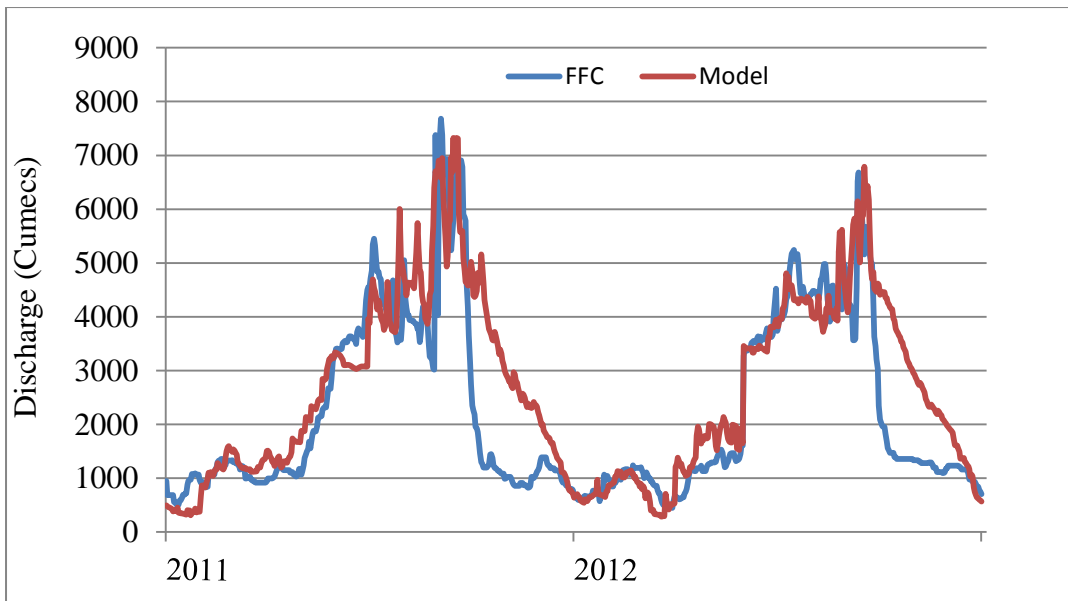


Figure 4.12. Validation results of SWAT model on Middle Indus River basin from 2011 and 2012.

Table 4.14. Model calibration and validation results with R² value, NSCE and Relative BIAS.

SWAT	R2 Value	NSCE	Relative BIAS
Calibration (2003-2010)	0.72	0.69	-0.06
Validation (2011-2012)	0.73	0.65	0.18

4.4 MODEL RUNOFF AND FLOOD INUNDATION MAPS

An important advantage of spatially semi-distributed hydrological models, such as SWAT, is that they not only provide estimates of hydrological variables at the basin outlet, but also at any location. SWAT model provides surface runoff to sub-watersheds which further divide into small units called hydrological response units (HRUs). This model produces surface runoff at each HRU on daily, monthly and yearly basis depends on user requirement. The runoff produced by the model at each HRU is in mm/day which represents two dimensional spread of precipitation over the area. A few rainy days were selected to display flood inundation maps of the study area. Flood inundation maps of three consecutive days 27, 28 and 29 July of 2010 with maximum rainfall of 56mm at 28th July and 8, 9 and 10 September of 2012 with maximum rainfall of 70mm at 9th September were generated. These maps show the runoff generated by precipitation that occurred within the study area. These maps show the areas of highly inundation as well as areas of less inundation on each day.

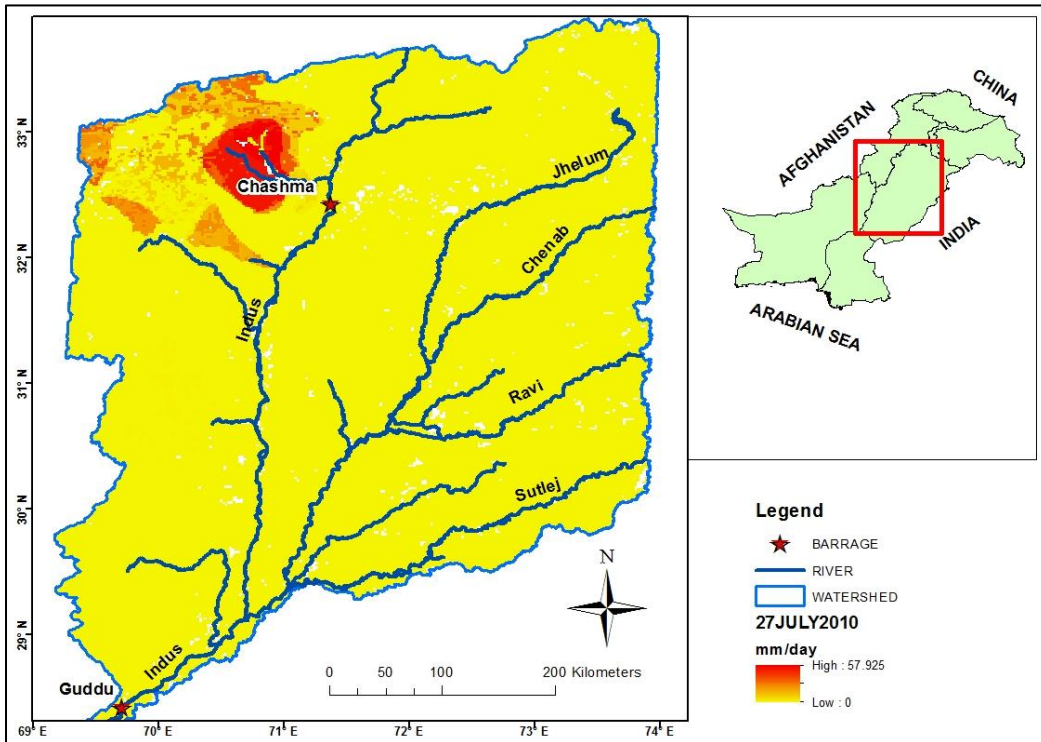


Figure 4.13. Runoff generated by SWAT for 27th July 2010 precipitation.

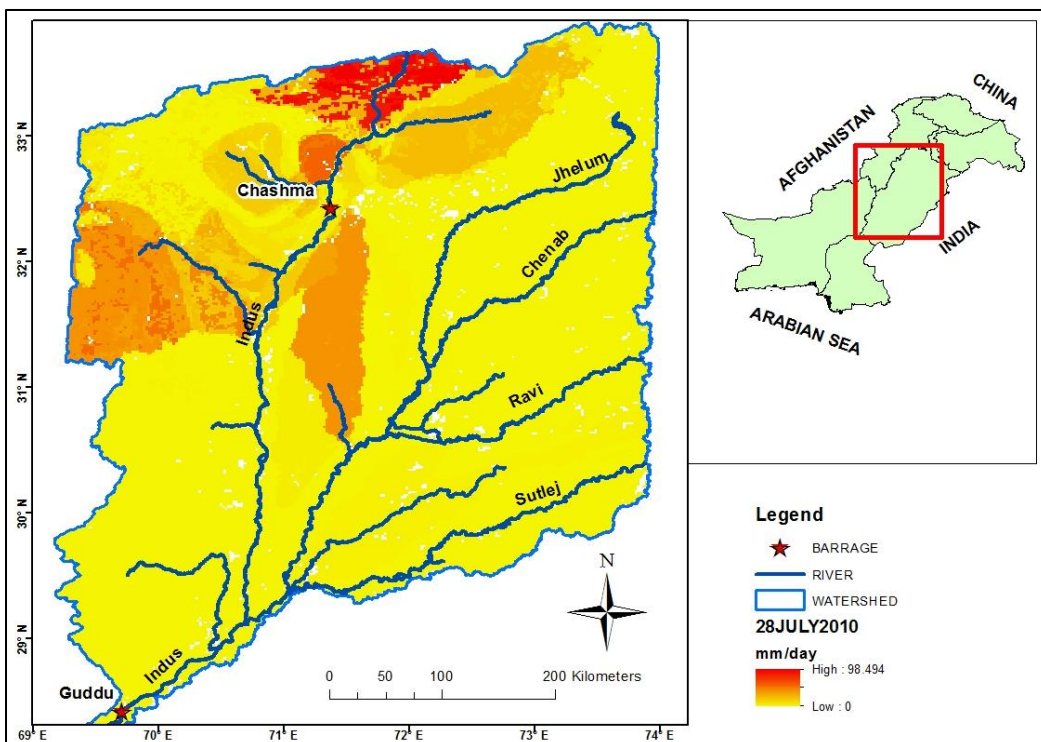


Figure 4.14. Runoff generated by SWAT for 28th July 2010 precipitation.

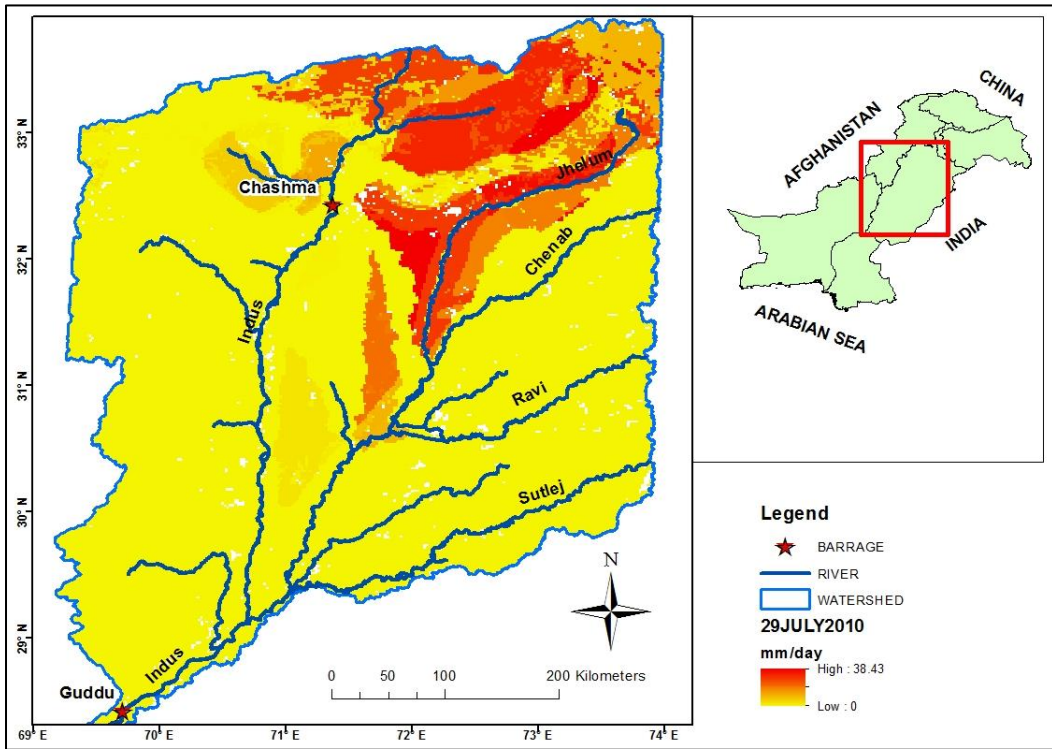


Figure 4.15. Runoff generated by SWAT for 29th July 2010 precipitation.

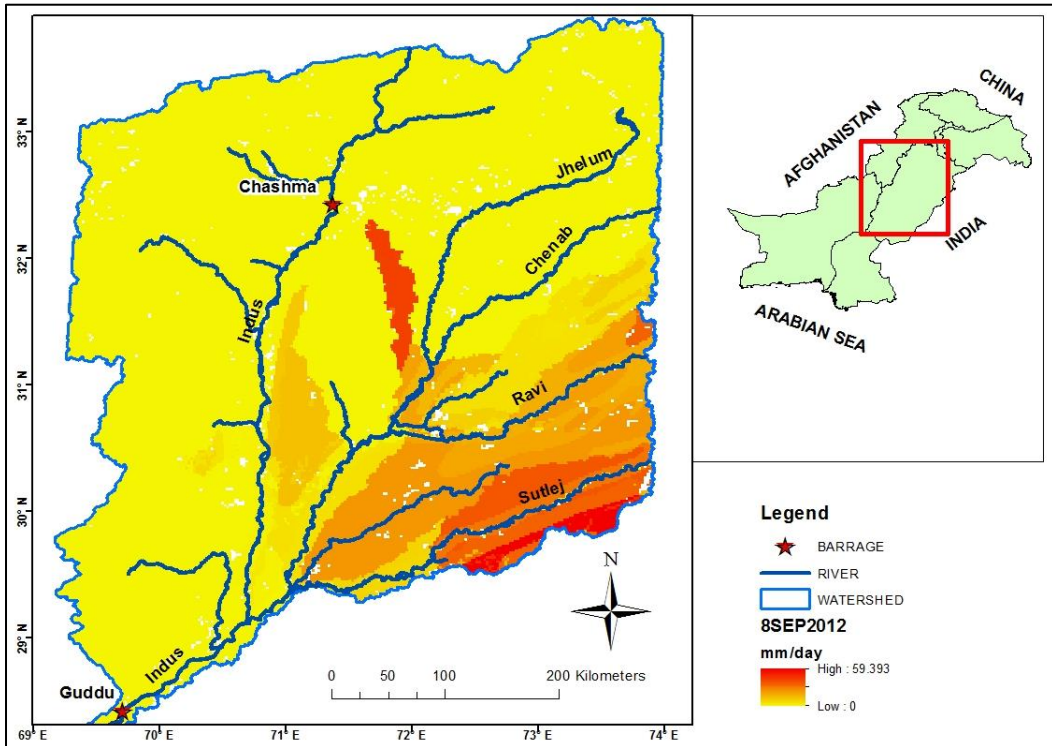


Figure 4.16. Runoff generated by SWAT for 8th September 2012 precipitation.

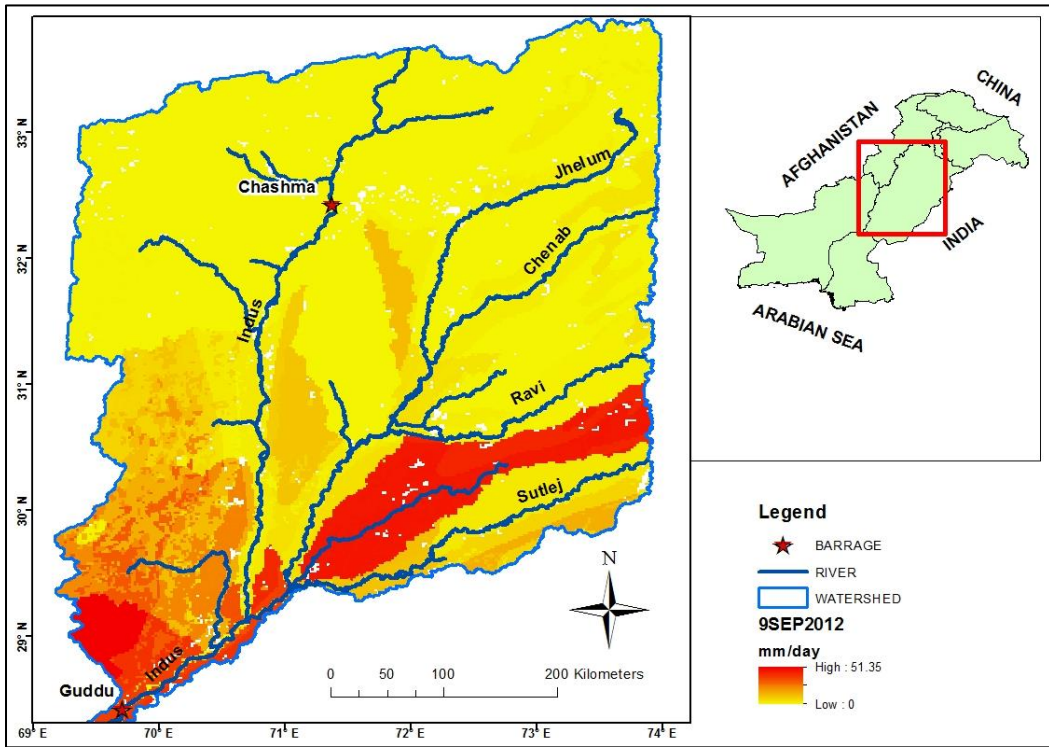


Figure 4.17. Runoff generated by SWAT for 9th September 2012 precipitation.

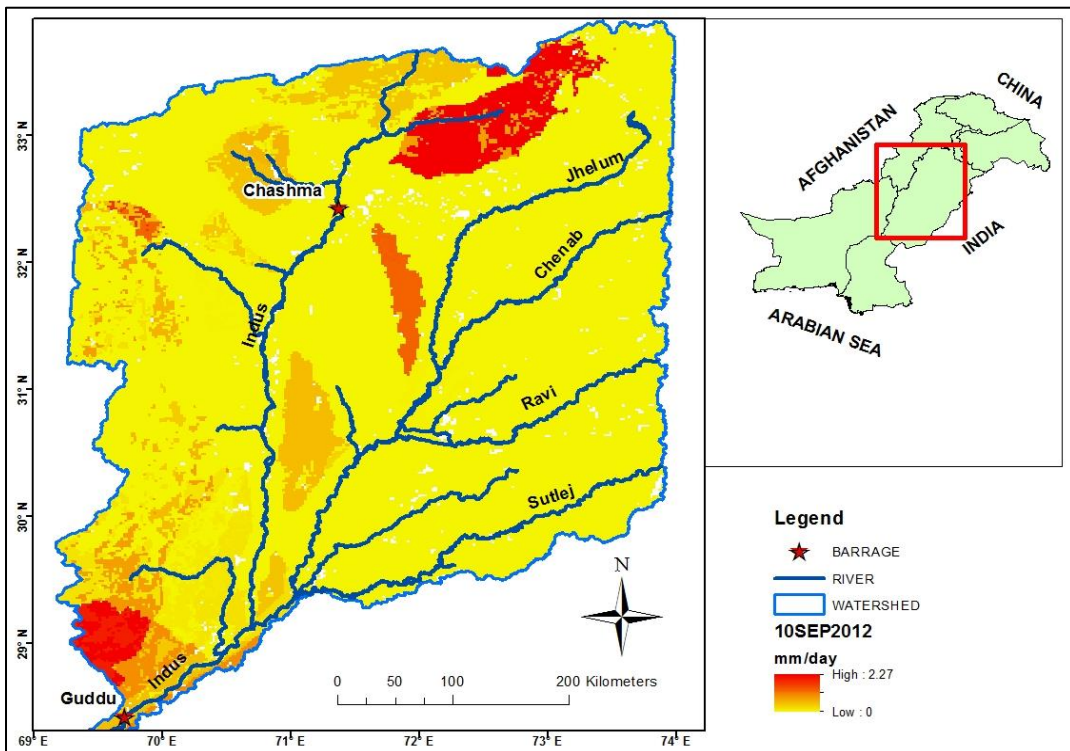


Figure 4.18. Runoff generated by SWAT for 10th September 2012 precipitation..

CONCLUSIONS AND RECOMENDATIONS

5.1 CONCLUSIONS

This research was carried out for flood inundation mapping of middle Indus river basin from Chashma to Guddu barrage by using SWAT model and satellite remotely sensed TRMM 3B42V7 precipitation data. In order to determine the accuracy of the satellite data to be used as a model input, the TRMM 3B42 V7 data was first validated statistically with in-situ gauged data of PMD. The comparison of TRMM with gauge data was done on daily and monthly basis. Daily rain comparison gave average values of CC= 0.64, RMSE= 4.69, Relative Bias%= -14 and $R^2= 0.42$ and monthly comparison with CC= 0.91, RMSE= 4.07, Relative Bias%= 26 and $R^2= 0.82$. This low value of R^2 in daily data comparison is mainly due to: (1) failure of TRMM estimates to capture local development of rainfall in monsoon and cyclic depression systems (2) difference in time of measurement of rain by PMD rain gauges and TRMM overpass (3) orographic, topographic and elevation impacts on the gauge and satellite estimates and (4) imperfections in the 3B42 V7 algorithm of the TRMM estimates in Himalayan terrain. If these two data sets captured rain at same time the difference should be minimized. The high CC and R^2 values in the monthly comparison indicate that the TRMM estimates have the potential to predict rain in the areas generally ungauged. It also indicates that the TRMM data can be used effectively in flood inundation and water resource management studies.

TRMM data from 2003 to 2012 was used as input parameter to SWAT hydrological model along with other input parameters like land cover, temperature and soil data etc. First eight years from 2003 to 2010 were used for model calibration and last two years 2011 and 2012 were used for model validation. The calibration and validation results with R^2 value=0.72 and 0.73, NSCE= 0.69 and 0.65 and Relative BIAS= -0.06 and 0.18 respectively, show that SWAT model can fairly accurately predict the river discharge at a water outlet point (e.g. Guddu barrage).

Flood inundation mapping was also done for selected precipitation events of years 2010 and 2012. The runoff generated at HRU level was mapped in 2D. The maps that were produced show the areas of high inundation as well as areas of low inundation. These maps can be very helpful for meteorological department and flood forecasting commission in their investigating of predicted climate change, floods, droughts and weather condition.

5.2 RECOMMENDATIONS FOR FURTHER RESESARCH

I recommend the use of high resolution DEM, Soil and Landover data in order to characterize more detailed HRUs. Compare and validate TRMM 3hourly data and use it instead of daily or monthly precipitation data. Use distributed models for analyzing the detail cell level routing and hydrology. Data should be available on finer spatial and temporal scale like meteorological parameters and discharge data. Other satellite estimates should be compared with TRMM estimates in order to authenticate its use more precisely. The runoff generated by the model should be compared with already generated flood extent maps of any Government or Non-Government organizations.

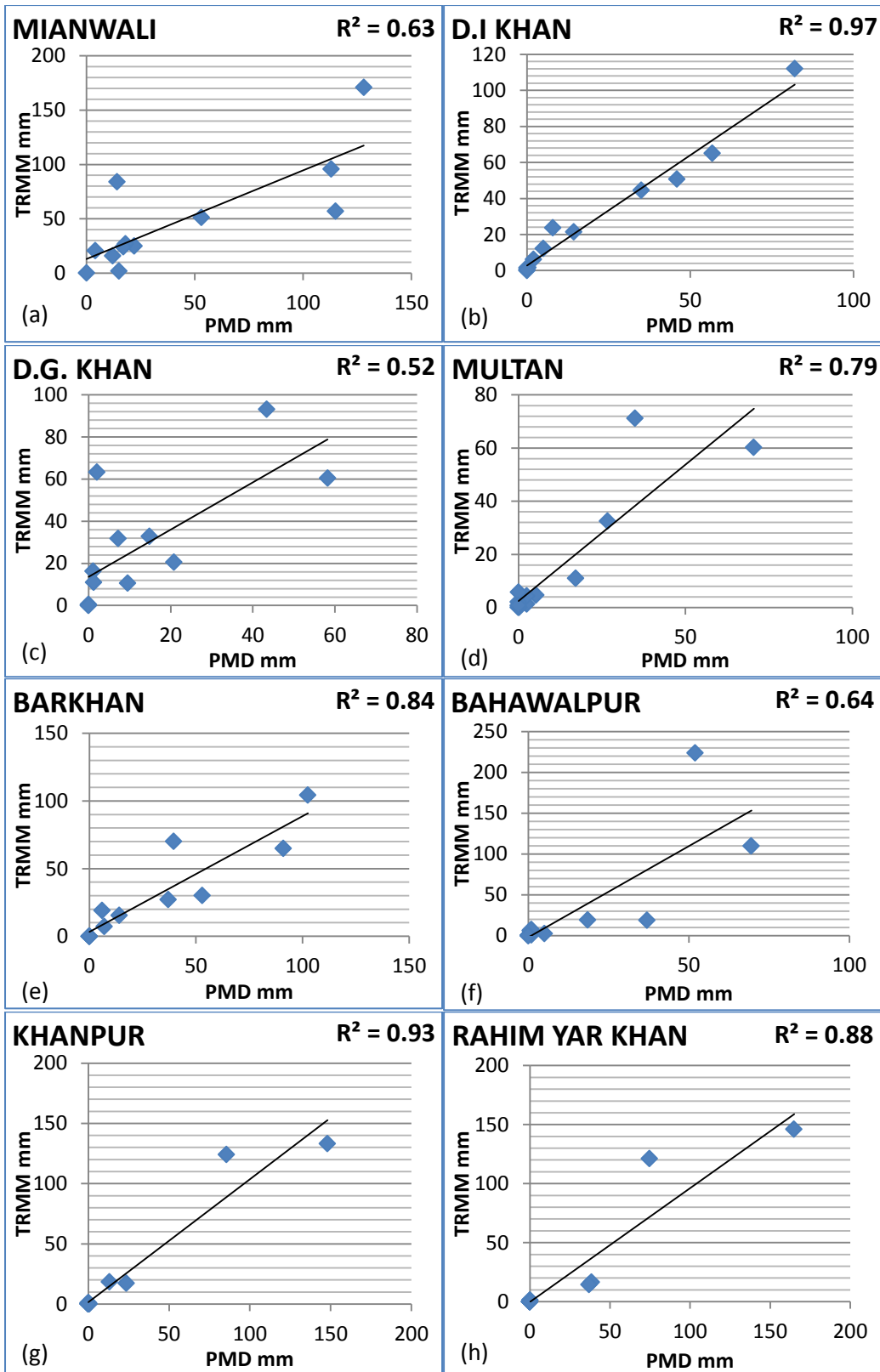
REFERENCES

- Arnell, N. W. (1999). A simple water balance model for the simulation of streamflow over a large geographic domain. *Journal of Hydrology*, 217(3), 314-335.
- Arnold, J., Williams, J., & Singh, V. (1995). SWRRB-a watershed scale model for soil and water resources management. *Computer models of watershed hydrology.*, 847-908.
- Artan, G., Gadain, H., Smith, J. L., Asante, K., Bandaragoda, C. J., & Verdin, J. P. (2007). Adequacy of satellite derived rainfall data for stream flow modeling. *Natural Hazards*, 43(2), 167-185.
- Barros, A., Joshi, M., Putkonen, J., & Burbank, D. (2000). A study of the 1999 monsoon rainfall in a mountainous region in central Nepal using TRMM products and rain gauge observations. *Geophysical Research Letters*, 27(22), 3683-3686.
- Bhatti, A. M., Suttinon, P., & Nasu, S. (2009). Agriculture water demand management in Pakistan: A review and perspective. *Society for Social Management Systems*, 1-7.
- Bolen, S. M., & Chandrasekar, V. (2003). Methodology for aligning and comparing spaceborne radar and ground-based radar observations. *Journal of Atmospheric & Oceanic Technology*, 20(5).
- Center, E. O. (2001). TRMM Data Users Handbook. *National Space Development Agency of Japan*.
- Chokngamwong, R., Chiu, L., 2006. TRMM and Thailand daily gauge rainfall comparison. . The 86th AMS Annual Meeting, Atlanta, GA, p. P1.2.
- Datta, S., Jones, W. L., Roy, B., & Tokay, A. (2003). Spatial variability of surface rainfall as observed from TRMM field campaign data. *Journal of Applied Meteorology*, 42(5).
- Döll, P., Kaspar, F., & Lehner, B. (2003). A global hydrological model for deriving water availability indicators: model tuning and validation. *Journal of Hydrology*, 270(1), 105-134.
- Gassman, P. W., Reyes, M. R., Green, C. H., & Arnold, J. G. (2007). *The soil and water assessment tool: historical development, applications, and future research directions*: Center for Agricultural and Rural Development, Iowa State University.
- Glossary of Meteorology. (2014). from American Meteorological Society <http://glossary.ametsoc.org/wiki/Rainfall>]
- Han, W. (2010). *Analysis of satellite rainfall data and global runoff process to improve global runoff modeling*. The University of Utah.
- Hong, Y., Adler, R. F., Hossain, F., Curtis, S., & Huffman, G. J. (2007). A first approach to global runoff simulation using satellite rainfall estimation. *Water resources research*, 43(8).
- Hong, Y., Adler, R. F., Negri, A., & Huffman, G. J. (2007). Flood and landslide applications of near real-time satellite rainfall products. *Natural Hazards*, 43(2), 285-294.

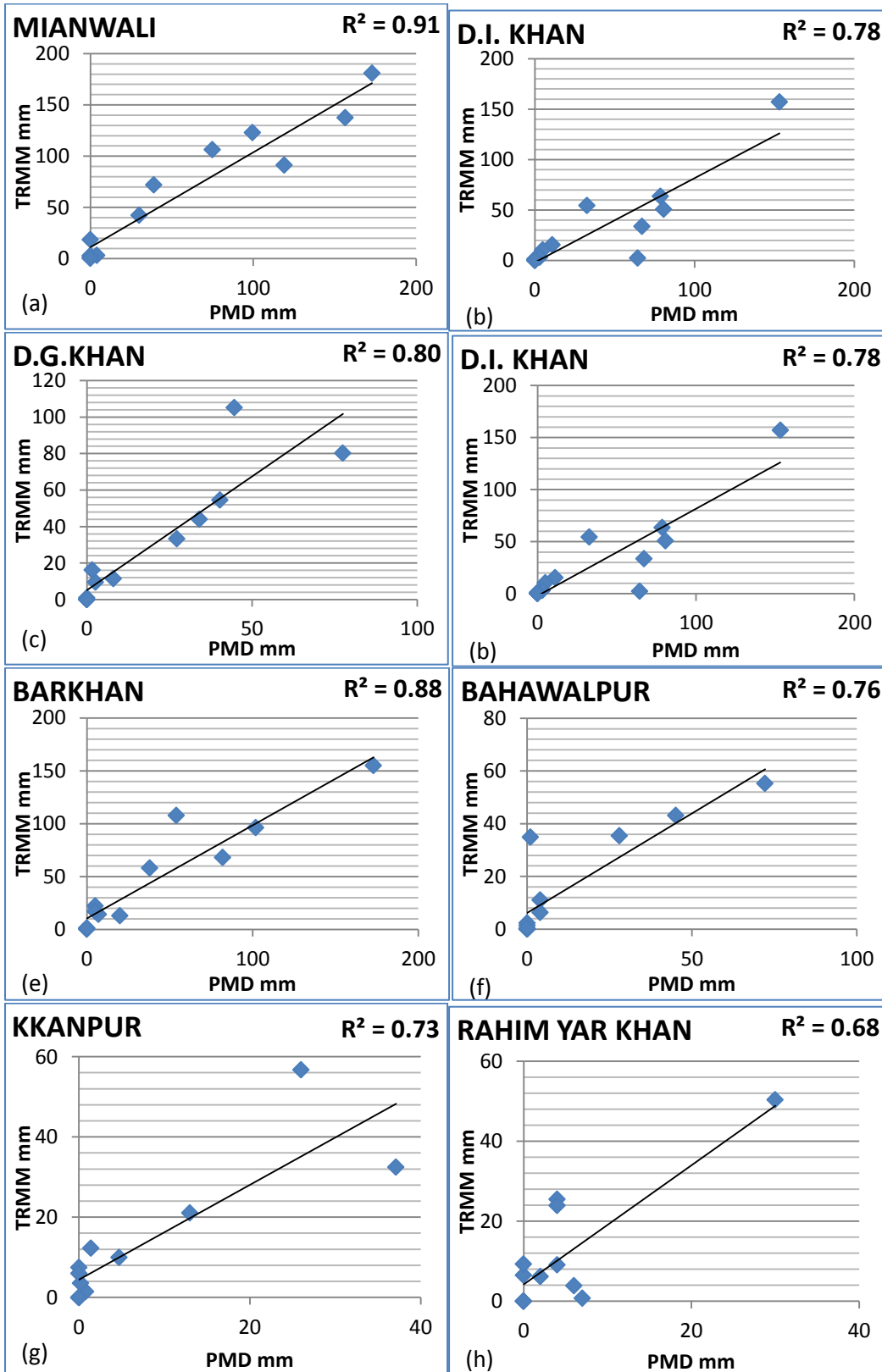
- Hossain, F., & Katiyar, N. (2006). Improving flood forecasting in international river basins. *Eos, Transactions American Geophysical Union*, 87(5), 49-54.
- Islam, M., & Uyeda, H. (2008). Vertical variations of rain intensity in different rainy periods in and around Bangladesh derived from TRMM observations. *International Journal of Climatology*, 28(2), 273-279.
- Ji, Y., & Stocker, E. (2003). *Ground validation of TRMM and AMSU microwave precipitation estimates*. Paper presented at the Geoscience and Remote Sensing Symposium, 2003. IGARSS'03. Proceedings. 2003 IEEE International.
- Khan, S. U., Hasan, M., Khan, F., & Bari, A. (2010). Climate classification of Pakistan. *Balwois-Ohrid, Republic of Macedonia, May*, 29.
- Klepper, O., & Van Drecht, G. (1998). WARiBaS, Water Assessment on a River Basin Scale. A computer program for calculating water demand and water satisfaction on a catchment basin level; to be used for global scale water stress analysis. *RIVM rapport 402001009*.
- Lakshmi, V. (2004). The role of satellite remote sensing in the prediction of ungauged basins. *Hydrological processes*, 18(5), 1029-1034.
- Lenhart, T., Eckhardt, K., Fohrer, N., & Frede, H.-G. (2002). Comparison of two different approaches of sensitivity analysis. *Physics and Chemistry of the Earth, Parts A/B/C*, 27(9), 645-654.
- Liu, X., Gao, T., & Liu, L. (2013). A comparison of rainfall measurements by multiple instruments. *Atmospheric Measurement Techniques Discussions*, 6(1).
- McCollum, J. R., Gruber, A., & Ba, M. B. (2000). Discrepancy between gauges and satellite estimates of rainfall in equatorial Africa. *Journal of Applied Meteorology*, 39(5), 666-679.
- Nash, J., & Sutcliffe, J. V. (1970). River flow forecasting through conceptual models part I—A discussion of principles. *Journal of hydrology*, 10(3), 282-290.
- Nicholson, S. E., Some, B., McCollum, J., Nelkin, E., Klotter, D., Berte, Y., Ndiaye, O. (2003). Validation of TRMM and other rainfall estimates with a high-density gauge dataset for West Africa. Part II: Validation of TRMM rainfall products. *Journal of Applied Meteorology*, 42(10).
- Nuystuen, J. A. (1999). Relative performance of automatic rain gauges under different rainfall conditions. *Journal of Atmospheric & Oceanic Technology*, 16(8).
- Nystuen, J. A., Proni, J. R., Black, P. G., & Wilkerson, J. C. (1996). A comparison of automatic rain gauges. *Journal of Atmospheric and Oceanic Technology*, 13(1), 62-73.
- Ohsaki, Y., Nakamura, K., & Takeda, T. (1999). Simulation-based error analysis on the comparison between rainfall rates measured by a spaceborne radar and by ground-based instruments. *Journal of the Meteorological Society of Japan*, 77(3), 673-686.
- Santhi, C., Arnold, J. G., Williams, J. R., Dugas, W. A., Srinivasan, R., & Hauck, L. M. (2001). VALIDATION OF THE SWAT MODEL ON A LARGE RWER BASIN WITH POINT AND NONPOINT SOURCES1: Wiley Online Library.

- Saw, B. L. (2005). *Infrared and passive microwave satellite rainfall estimate over tropics*. University of Missouri.
- Sharma, R., Samarkoon, L., Hazarika, M., & Kafle, T. (2007). Applicability of tropical rainfall measuring mission to predict floods on the Bagmati River. *J Hydrol Meteorol*, 4(1), 1-15.
- Shrestha, M., Artan, G., Bajracharya, S., & Sharma, R. (2008). Using satellite-based rainfall estimates for streamflow modelling: Bagmati Basin. *Journal of Flood Risk Management*, 1(2), 89-99.
- Tech, T. (2013). *Lake Champlain Basin SWAT Model Configuration, Calibration and Validation*.
- Van Griensven, A., Francos, A., & Bauwens, W. (2002). Sensitivity analysis and auto-calibration of an integral dynamic model for river water quality. *Water Science & Technology*, 45(9), 325-332.
- Vorosmarty, C. J., Moore, B., Grace, A. L., Gildea, M. P., Melillo, J. M., Peterson, B. J., . . . Steudler, P. A. (1989). Continental scale models of water balance and fluvial transport: An application to South America. *Global biogeochemical cycles*, 3(3), 241-265.
- Wolff, D. B., Marks, D., Amitai, E., Silberstein, D., Fisher, B., Tokay, A., . . . Pippitt, J. (2005). Ground validation for the Tropical Rainfall Measuring Mission (TRMM). *Journal of Atmospheric & Oceanic Technology*, 22(4).
- Yilmaz, L. (2005). *Space in the service of prediction hydrological data, RAST 2005*. Paper presented at the Proceedings of 2nd international conference on recent advances in space technologies, Istanbul, Turkey.
- Zhou, T., Yu, R., Chen, H., Dai, A., & Pan, Y. (2008). Summer precipitation frequency, intensity, and diurnal cycle over China: A comparison of satellite data with rain gauge observations. *Journal of Climate*, 21(16).

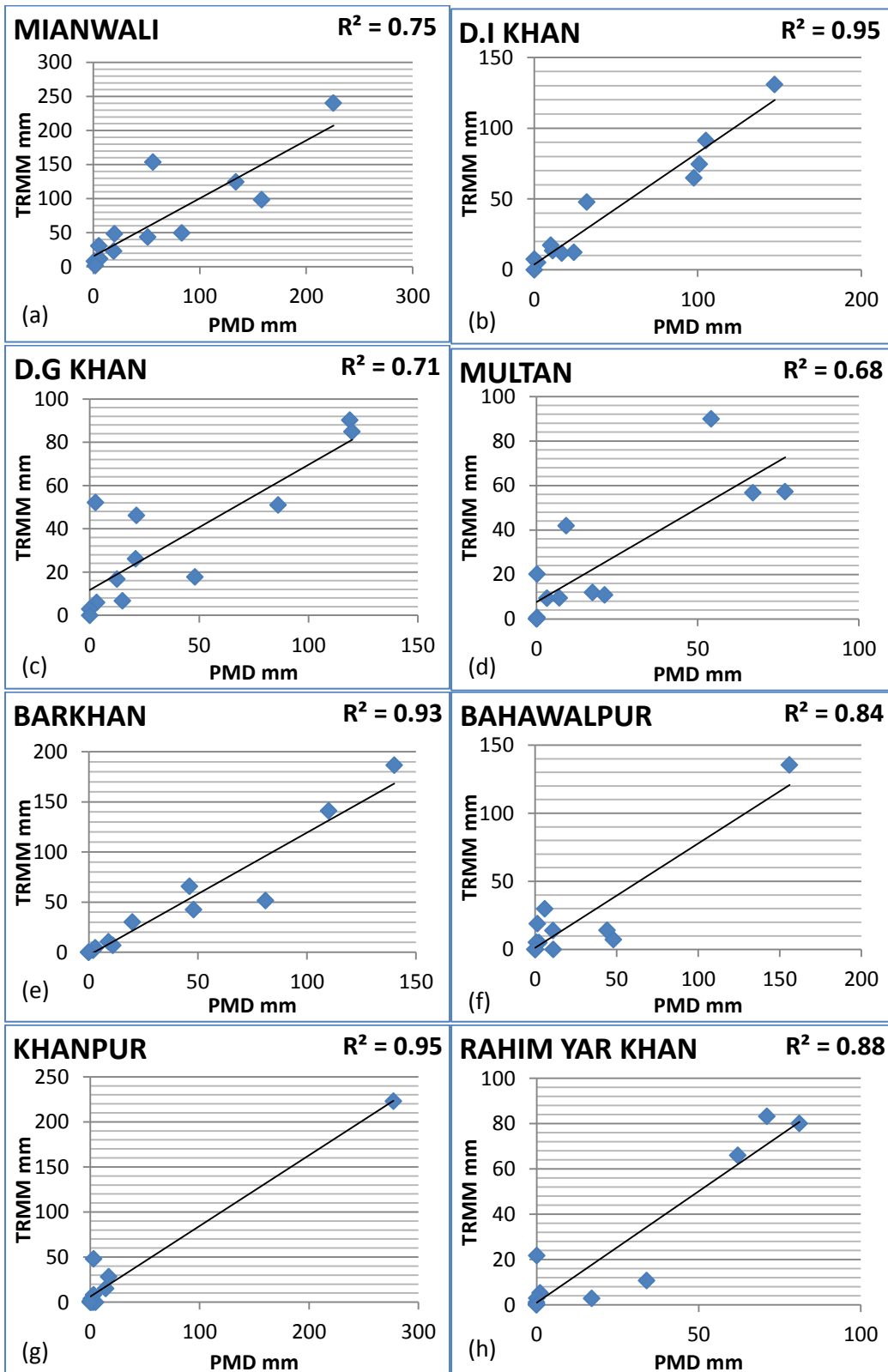
APPENDICES



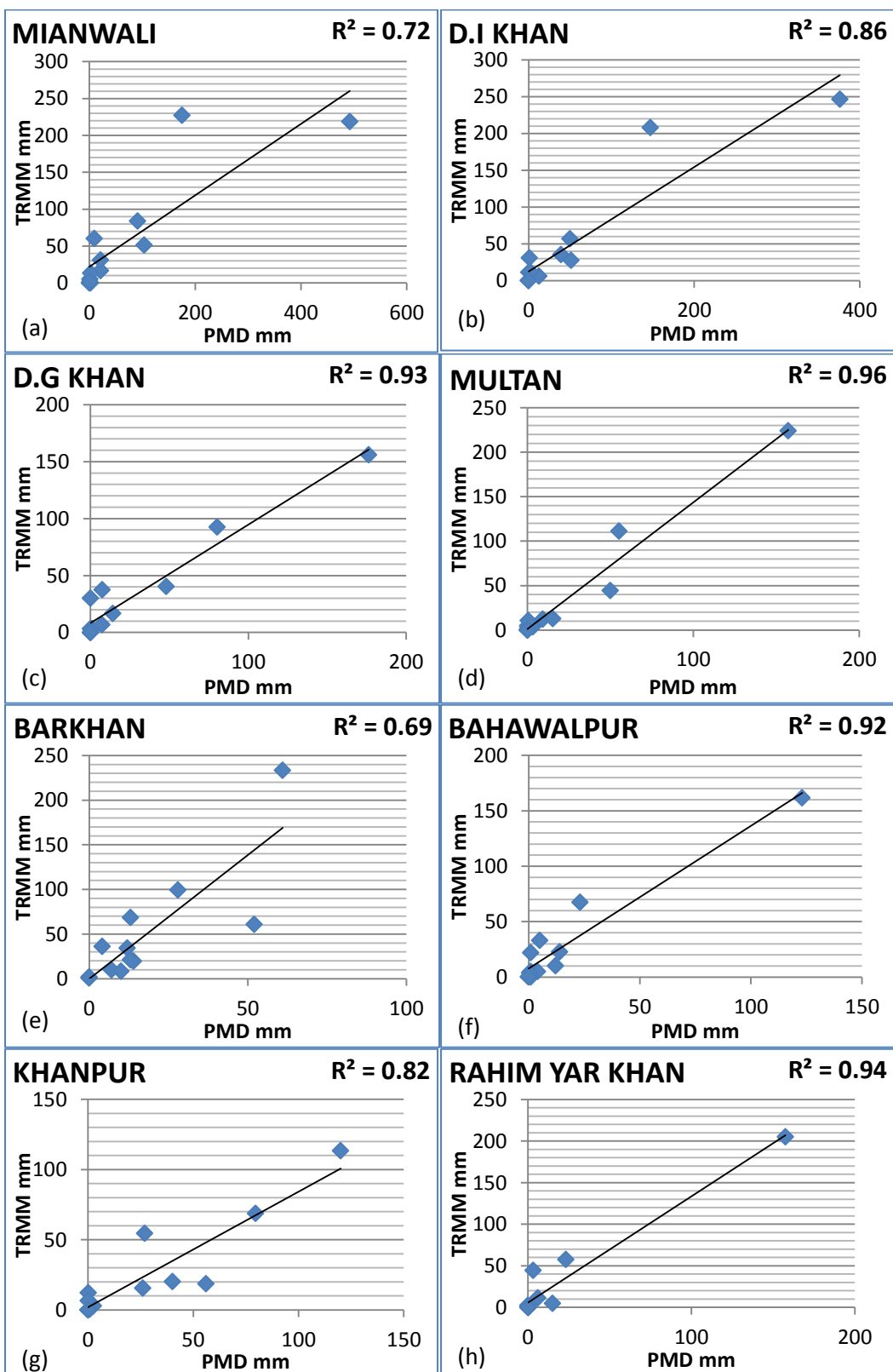
Appendix 1. Scatter plots with regression line of monthly TRMM vs PMD data of year 2003 (n=365).



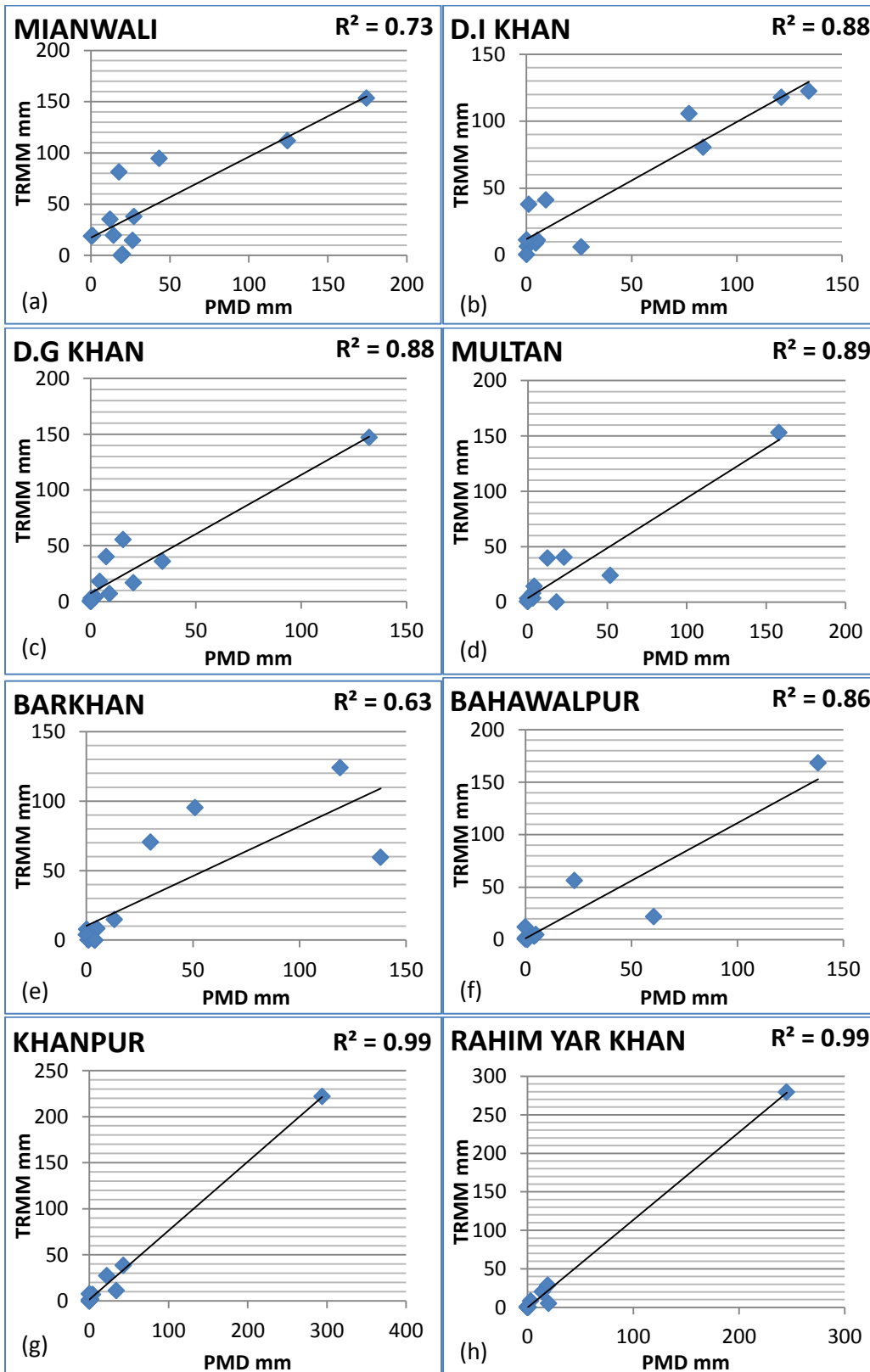
Appendix 2. Scatter plots with regression line of monthly TRMM vs PMD data of year 2005 (n=365).



Appendix 3. Scatter plots with regression line of monthly TRMM vs PMD data of year 2008 (n=366).



Appendix 4. Scatter plots with regression line of monthly TRMM vs PMD data of year 2010 (n=365).



Appendix 5. Scatter plots with regression line of monthly TRMM vs PMD data of year 2012 (n=366).